KEYNOTE
PERKIN 2

MCD of non-aromatic cyclic π-electron systems. Part 1. The perimeter model for antiaromatic 4*N*-electron [*n*]annulene biradicals[1]

Udo Höweler, John W. Downing, Jörg Fleischhauer † and Josef Michl*

Department of Chemistry and Biochemistry, University of Colorado, Boulder, CO 80309-0215, USA

The LCAO version of the perimeter model with overlap through second order is used to obtain algebraic solutions for the singlet electronic states of the antiaromatic 4*N*-electron [*n*]annulenes of D_{nh} symmetry. The states of these biradicals are classified and their spectroscopic properties derived. General simple results are given for the signs and magnitudes of the *A*, *B* and *C* terms in magnetic circular dichroism. The effects of perturbations that preserve the antiaromatic biradical or biradicaloid character are considered. Other perturbations will be treated in Parts 2 and 3.

1. Introduction

Paul Dowd, to whose memory this paper is dedicated, played an essential role in developing the contemporary understanding of the properties of biradicals. These usually highly reactive species are well recognized as crucial intermediates in many thermal and photochemical processes and as fundamental building blocks in the design of organic magnetic materials. Here, we turn to another important facet of biradical chemistry, namely to their use as important paradigms of electronic structure.

Specifically, we shall deal with 4*N*-electron [*n*]annulenes, expected to be perfect biradicals at their most symmetrical D_{nh} geometries. Although they are of limited practical significance themselves, their electronic structure is of considerable theoretical interest since they are the focal points for the understanding, classification and organization of the electronic states of a large number of related compounds that are not biradicals, and for the prediction of trends in their properties.

Although high-quality *ab initio* computations of a large number of states for many individual compounds are helpful, systematic state correlations, classification, and qualitative understanding of trends are most easily obtained from simple models that allow algebraic solutions for families of compounds. The models are only useful if they contain all of the relevant physics and if they agree at least qualitatively with the more sophisticated calculations where the latter are available. In a sense, at least for a limited number of low-energy states, the simple models allow us to understand why the *ab initio* computations provide the answers they give.

A classical example of a simple algebraically soluble model that provided a great deal of qualitative understanding, spectral interpretations and predictions for the electronic states of a large family of compounds is the perimeter model of cyclic π-electron systems derived from (4*N* + 2)-electron [*n*]annulenes. This was originally developed by Platt in the free-electron form[2] and cast by Moffitt into the LCAO form.[3] It provided an early understanding of the systematics of low-lying electronic states of aromatic molecules such as the polyacenes,[2,3,4,5] azulenes[6] and porphyrins.[7] The ability of this model to correlate trends in transition energies, intensities and polarizations of a vast group of organic compounds is remarkable. It also introduced the L_b, L_a, B_b, B_a state notation, commonly used to the present day. This notation represents a valuable complement to the group theoretical notation, since it transcends a huge diversity of structural variations.

It is known[8,9,10] that only a minor refinement with respect to the treatment of overlap is needed to extend the perimeter model to the interpretation of absolute signs in magnetic circular dichroism (MCD). By now, a simple set of rules derived from the perimeter model has accounted for hundreds of MCD signs in the spectra of all kinds of aromatic π-systems, *i.e.* those derived from a (4*N* + 2)-electron perimeter.[11] The trends and regularities in the effects of substitution, heteroatom replacement, and other structural changes on these signs can be simply understood and/or predicted in an *a priori* fashion without recourse to numerical computations.

These results and the Platt notation are not applicable to cyclic even-electron chromophores that cannot be derived by perturbation of a (4*N* + 2)-electron perimeter. In the present series of papers we ask whether the perimeter model can account for the electronic properties and the MCD signs of singlet ground state cyclic π-electron systems derivable from the 'antiaromatic' D_{nh}-symmetry 4*N*-electron [*n*]annulene perimeters, which are of biradical nature, and whether it again leads to useful predictions and to a systematic nomenclature, generally applicable regardless of structural types. Such a nomenclature presently does not exist for π-electron chromophores derived from this type of perimeter. Triplet states will have to be dealt with separately.

Chart 1 displays the relations between the terms we propose to use for the classification of even-electron cyclic π-systems for the purposes of electronic and, in particular, MCD spectroscopy. The concepts of D_{nh}-symmetry parent aromatic (4*N* + 2)-electron [*n*]annulene and antiaromatic 4*N*-electron [*n*]annulene perimeters are well established. We now propose to use the terms *aromatic* and *nonaromatic*, and three subdivisions of the latter category, *ambiaromatic*, *antiaromatic* and *unaromatic*, to describe all those systems formally obtainable from a D_{nh} polygon [*n*]annulene perimeter by cross-linking, bridging (in Chart 1, once by union with $\rangle C^+-$ and once with $\rangle C^--$), heteroatom replacement and substitution. Although uncommon, this nomenclature is space-saving and convenient for the present purpose.

Aromatic π-systems

In the past we used the term 'aromatic' for all systems derivable from (4*N* + 2)-electron perimeters. Except perhaps in some cases of very strongly perturbed perimeters such as uracil, this coincided fairly well with the common usage of the term. We now need to restrict the term aromatic to those cyclic π systems

† *Permanent address:* Institut für Organische Chemie, RWTH Aachen, Prof.-Pirlet-Str.1, D-52056 Aachen, Germany.

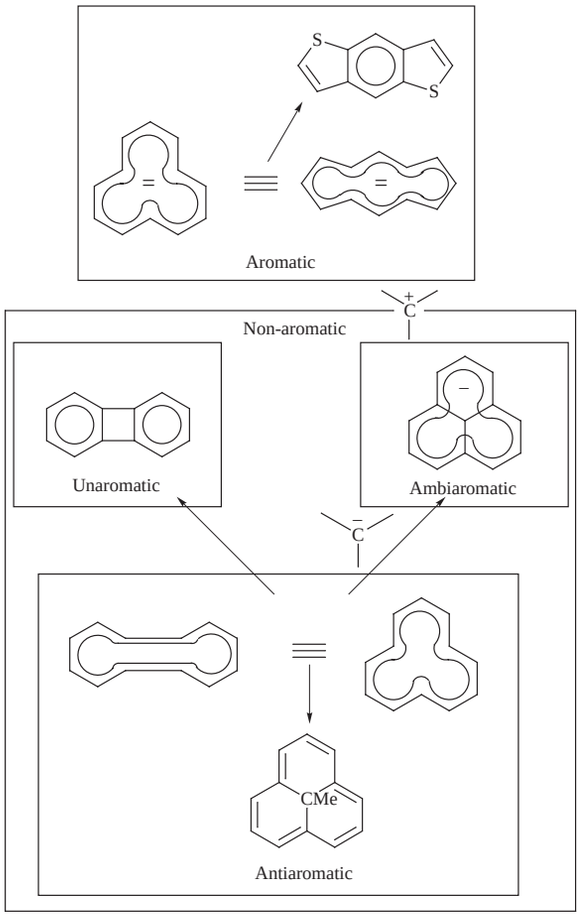

Chart 1 Classification of even-electron cyclic π systems for the purposes of electronic spectroscopy

that can be derived from a $(4N + 2)$-electron perimeter but cannot be derived equally well from a $4N$-electron perimeter. This will exclude molecules such as the phenalenide anion (**1**) or acenaphthylene (**2**) from the aromatic category.

1 **2**

Non-aromatic cyclic π systems

We use the expression 'non-aromatic cyclic π system' to describe all π-electron systems that can be derived from a $4N$-electron perimeter, regardless of whether they are ambiaromatic, antiaromatic or unaromatic. To some readers, the word 'non-aromatic' may imply acyclic conjugation or no conjugation unless explicitly specified otherwise, but this is not our usage of the term.

(i) Ambiaromatic. Those cyclic π systems that can be derived equally well from both $(4N + 2)$-electron and $4N$-electron perimeters, such as **1** and **2**, are called ambiaromatic to indicate the ambiguous nature of their electronic state labels, with two alternative sets of labels equally justified.

(ii) Antiaromatic. It would be misleading to refer to all systems that are derivable only from an antiaromatic $4N$-electron annulene as antiaromatic since many, such as biphenylene, exhibit significant resonance stabilization and the term antiaromatic already has a well established specific meaning which precludes that. Thus, we use the term antiaromatic only for the $4N$-electron annulene perimeters of D_{nh} symmetry and for those cyclic π-electron systems that are derivable from them [but not equally well from a $(4N + 2)$ perimeter] that still have very strong biradical-like character, like the parent annulenes. As will be shown in Part 2, the distinction can be made quite clear and quantitative within the two-electrons-in-two-orbitals (3×3 CI) approximation for the ground state. This definition of 'antiaromatic' is very restrictive and very few, if any, known singlet molecules have equilibrium ground-state structures that satisfy the requirement, due to the occurrence of Jahn–Teller and pseudo-Jahn–Teller distortions.

(iii) Unaromatic. We then need another term to describe cyclic π-electron systems derivable from a $4N$-electron [n]annulene perimeter [but not equally well from a $(4N + 2)$-electron perimeter] by perturbations that are strong enough to remove biradical-like character (*e.g.* biphenylene, pentalene, *p*-benzoquinone). We have decided to adopt the term unaromatic, which does not appear to have been pre-empted.

Note that in our usage the terms aromatic, ambiaromatic, antiaromatic and unaromatic are primarily meant to provide formal information about the structural formula only. Their relation to molecular stability, reactivity, ring current, *etc.*, is only indirect insofar as these properties are determined once a structural formula is specified.

The purpose in defining the various categories of even-electron cyclic systems is to identify unambiguously the range of applicability of the four systems of electron singlet state classification that we shall arrive at in our attempt to make general statements about intensities, polarizations, and above all, MCD signs of electronic transitions. In addition to the lowest singlet state G, we shall have the following low-energy singlet electronic states: (i) aromatic systems: L_b, L_a, B_b, B_a (uncharged perimeters, $n = 4N + 2$)[3,5,6] or L_1, L_2, B_1, B_2 (charged perimeters, $n \neq 4N + 2$);[7–10] (ii) antiaromatic (biradical) systems: modified irreducible representation symbols such as $B^{(+)}$, $B^{(-)}$, $E^{(-)}_{2N+1}$ *etc.*, and in the special case of certain high symmetry perturbations: S, D, N, N′, P, P′ (Part 1 of this series); (iii) unaromatic systems: S, D, N_1, N_2, P_1, P_2 (Parts 2 and 3 of this series); (iv) ambiaromatic systems: labels from (i) and (iii) are both equally applicable (Parts 2 and 3 of this series).

Two distinct nomenclature systems for the antiaromatic and the unaromatic systems derived from uncharged perimeters are needed since there is no one-to-one correspondence between the two, due to the presence of a conical intersection of the lowest two singlet surfaces (Part 2). Categories (ii), (iii) and (iv) together are referred to as cyclic non-aromatic in the title of the present series of papers. Aromatic systems (i) have been handled in a previous series of papers.[8,9,10,11]

In Part 1 of this series, we describe the results of the perimeter model for the MCD spectra of antiaromatic [n]annulenes at their ideal D_{nh} symmetry, at which they are perfect biradicals, and of those of their perturbed analogs that are still antiaromatic, *i.e.* are perfect biradicals or at least biradicaloids. Uncharged ($4N = n$) and charged ($4N \neq n$) perimeters need to be treated separately. The former are 'pair biradicals' and the latter are 'axial biradicals' in the sense of ref. 12.

We find simple results only for those systems in which the highest fully occupied MO and the lowest completely unoccupied MO are degenerate, *i.e.*, the parent [n]annulenes of D_{nh} symmetry and some high-symmetry alternant biradicaloids. In some other cases, the results can be written explicitly as well but are too complicated to offer insight without a numerical calculation. This will not matter much in practice; although an appreciation of the case of antiaromatic systems is a prerequisite for the understanding of the unaromatic ones, in practice the former will be rarely, if ever, encountered.

In Parts 2 and 3, we will consider unaromatic π systems, *i.e.* those derived from the parent antiaromatic D_{nh} [n]annulene perimeters by stronger perturbations (*e.g.* Chart 1). As indicated above, for these, a general classification and simple rules for MCD signs as a function of molecular structure are obtained.

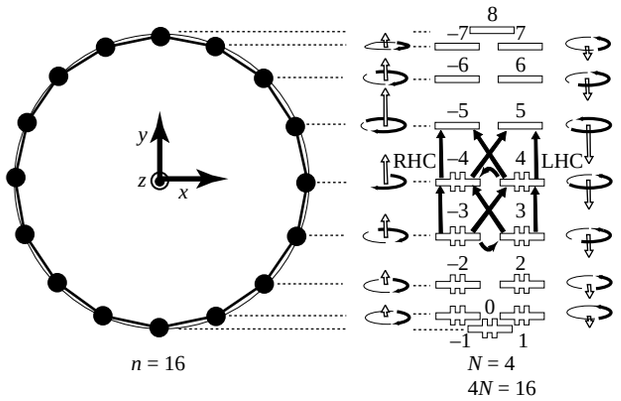

Fig. 1 Left, the coordinate system and the assumed geometry of a regular [*n*]annulene perimeter. Right, electron occupancy in the configuration Ψ_0 of a 4*N*-electron [*n*]annulene. The orbitals are labeled by the subscript *k* of the irreducible representation ε_k in the C_{16} symmetry group. The dominant sense of angular electron motion is indicated schematically and the *z* component of the resulting orbital magnetic moment is shown by a white arrow. The ten single excitations under consideration are shown as dark arrows. The vertical arrows correspond to excitations which require left-handed (LHC) or right-handed (RHC) circularly polarized light as shown, the other transitions are forbidden.

Their use is illustrated on two ambiaromatic systems whose MCD spectra have already been discussed earlier in terms of the Platt L, B nomenclature, applicable to aromatic π systems. In subsequent papers of the series, we will apply the results to several other classes of unaromatic compounds.

2. The perimeter model

The formulation of the perimeter model for 4*N*-electron [*n*]-annulenes follows closely the pattern set up for (4*N* + 2)-electron [*n*]annulenes,[10] and only the nature and properties of the many-electron configurations and states are different. In particular, (i) we adopt the zero-differential-overlap (ZDO) approximation for Löwdin-orthogonalized atomic orbitals, (ii) we keep only the nearest-neighbor resonance integrals β_1 between these orthogonalized AOs in the evaluation of energy terms, so the pairing theorem applies for alternant (even) perimeters, (iii) for the magnetic moment operator $\hat{\boldsymbol{\mu}}$ both the nearest and the next-nearest neighbor matrix elements in the orthogonalized AO basis are kept, for reasons explained in the next section. On several occasions, we point out simplifications in the results that are obtained when only the nearest neighbor matrix elements of $\hat{\boldsymbol{\mu}}$ are kept ('perfect alternant pairing approximation').

AO basis

For the π system of a parent D_{nh} 4*N*-electron [*n*]annulene, we define a basis set of *n* non-orthogonal $2p_z$ atomic orbitals labeled 0 to *n*–1 and located at the vertices of a regular polygon whose center is at the origin of a right-handed coordinate system characterized by the unit vectors ***x***, ***y*** and ***z***, with ***x*** going through atom 0 and ***z*** directed perpendicular to the polygon (Fig. 1). The matrix elements of the single-electron electric ($\hat{\boldsymbol{m}}$) and magnetic ($\hat{\boldsymbol{\mu}}$) dipole moment operators are defined in this basis according to ref. 8. These AOs are subject to an explicit Löwdin orthogonalization,[13] considering overlap integrals only through second order. The ratio of the matrix elements of $\hat{\mu}_z$ between next-nearest-neighbor AOs to that for nearest-neighbor AOs is set to −0.15 as justified by direct integration for STOs.[8]

MO basis

The complex MOs , eqn. (1), are obtained by symmetry adaptation of the Löwdin orbitals χ_ν to the *n*-fold axis of symmetry. The index *k* denotes the orbital angular momentum 'quantum numbers' as well as the label of the irreducible representation ε_k of the C_n symmetry group according to which ψ_k transforms. The energy of the orbitals increases with increasing absolute value of *k* as indicated in Fig. 1.

$$\psi_k = n^{-1/2} \sum_{\nu=0}^{n-1} [\exp(2\pi i k\nu/n)]\, \chi_\nu \qquad (1)$$

The non-vanishing matrix elements of the electric and magnetic dipole moment operators in the MO basis are:[8]

$$\langle \psi_k | \hat{\boldsymbol{m}} | \psi_{k\pm1} \rangle = m(n, |2k \pm 1|)(\boldsymbol{x} \pm i\boldsymbol{y})/\sqrt{2} \qquad (2)$$

$$\langle \psi_k | \hat{\boldsymbol{\mu}} | \psi_k \rangle = \mu(n,k)\boldsymbol{z} \qquad (3)$$

the values of $m(i,j)$ are:

$$m(3,1) = -el_0\,(1 + 9S^2/8)/\sqrt{6} \qquad (4)$$

$$m(4,1) = m(4,3) = -el_0(1 + S^2/2)/2 \qquad (5)$$

$$m(n,j) = [(-el_0/2\sqrt{2})\sin(\pi/n)][1 + 2S^2 \sin^2(\pi/n) \sin^2(\pi j/n)] \quad \text{for } n > 4 \qquad (6)$$

the values of $\mu(n,k)$ are:

$$\mu(3,\pm1) = \mp|\beta_1|(m\beta_e l_0^2/2\hbar^2)(1 + S) \qquad (7)$$

$$\mu(n,k) = -|\beta_1|(m\beta_e l_0^2/\hbar^2)\cos(\pi/n)[\sin(2\pi k/n) - 0.15 \sin(4\pi k/n)] \quad \text{for } n > 3 \qquad (8)$$

where *e* and *m* are the magnitudes of the electron charge and mass, l_0 is the distance between neighboring AOs, *S* is their overlap integral, $|\beta_1|$ is the magnitude of the resonance integral for nearest neighbors and β_e is the Bohr magneton. The electric dipole moment integrals vanish except for transitions which change *k* by unity and the magnetic dipole moment operator is diagonal, with positive moments for $k < 0$ and negative ones for $k > 0$, as shown in Fig. 1. The magnitudes $m(n,|2k \pm 1|)$ and $\mu(n,k)$ are characteristic of perimeter size and charge.[8] The factor −0.15 in eqn. (8) results from the sign and estimated size of the next-nearest neighbor resonance integral relative to the usual nearest-neighbor resonance integral. This estimate[8] is supported by recent *ab initio* evaluations of this semiempirical parameter.[14]

Configuration state function basis

Only the MOs ψ_{N-1}, ψ_{-N+1} (the highest fully occupied level of the ground configuration, HO), ψ_N, ψ_{-N} (the level of singly occupied orbitals, SO) and ψ_{N+1}, ψ_{-N-1} (the lowest completely unoccupied level, LO) are considered in the generation of the active singlet configuration space (Fig. 1). In the following we shall need to refer to the average energy of the HO orbital pair ψ_{N-1}, ψ_{-N+1} as *E*(HO), the average energy of the SO orbital pair ψ_N, ψ_{-N} as *E*(SO) and the average energy of the LO orbital pair ψ_{N+1}, ψ_{-N-1} as *E*(LO). In this context, the orbital energies refer to the one-electron part of the Hamiltonian only.

The reference singlet configuration is $\Psi_0 = {}^1|\psi_0^2\psi_1^2\psi_{-1}^2 \ldots \psi_{N-1}^2\psi_{-N+1}^2\psi_N^1\psi_{-N}^1\rangle$ (Fig. 2). In the general case, ten singlet configurations related to it by single excitations are considered. Restricting the configuration basis to these few single excitations is justified by the fact that other excitations are both of higher energy and have vanishing or nearly vanishing electric dipole transition moments from Ψ_0. We use notation Ψ_k^l for a singlet excitation from ψ_k to ψ_l.

The configurations Ψ_{-N}^N and Ψ_N^{-N} arise from excitations with-

Table 1 Configurations and their properties

	Configuration	Symmetry[a]	Magnetic moment
Ψ_0	$^1\|\psi_0\bar{\psi}_0 \ldots \psi_N\bar{\psi}_{-N}\rangle$	ε_0	0
Ψ_{-N}^{N}	$^1\|\psi_0\bar{\psi}_0 \ldots \psi_N\bar{\psi}_N\rangle$	ε_{2N}	$2\mu(n,N)$
Ψ_{N}^{-N}	$^1\|\psi_0\bar{\psi}_0 \ldots \psi_{-N}\bar{\psi}_{-N}\rangle$	ε_{-2N}	$-2\mu(n,N)$
Ψ_{N}^{N+1}	$^1\|\psi_0\bar{\psi}_0 \ldots \psi_{-N}\bar{\psi}_{N+1}\rangle$	ε_1	$\mu(n,N+1) - \mu(n,N)$
Ψ_{-N}^{-N-1}	$^1\|\psi_0\bar{\psi}_0 \ldots \psi_N\bar{\psi}_{-N-1}\rangle$	ε_{-1}	$-\mu(n,N+1) + \mu(n,N)$
Ψ_{N-1}^{N}	$^1\|\psi_0\bar{\psi}_0 \ldots \psi_N\bar{\psi}_N\psi_{N-1}\bar{\psi}_{-N}\rangle$	ε_1	$\mu(n,N) - \mu(n,N-1)$
Ψ_{-N+1}^{-N}	$^1\|\psi_0\bar{\psi}_0 \ldots \psi_{-N}\bar{\psi}_{-N}\psi_{-N+1}\bar{\psi}_N\rangle$	ε_{-1}	$-\mu(n,N) + \mu(n,N-1)$
Ψ_{N}^{-N-1}	$^1\|\psi_0\bar{\psi}_0 \ldots \psi_{-N}\bar{\psi}_{-N-1}\rangle$	ε_{-2N-1}	$-\mu(n,N+1) - \mu(n,N)$
Ψ_{-N}^{N+1}	$^1\|\psi_0\bar{\psi}_0 \ldots \psi_N\bar{\psi}_{N+1}\rangle$	ε_{2N+1}	$\mu(n,N+1) + \mu(n,N)$
Ψ_{-N+1}^{N}	$^1\|\psi_0\bar{\psi}_0 \ldots \psi_N\bar{\psi}_N\psi_{-N+1}\bar{\psi}_{-N}\rangle$	ε_{2N-1}	$\mu(n,N) + \mu(n,N-1)$
Ψ_{N-1}^{-N}	$^1\|\psi_0\bar{\psi}_0 \ldots \psi_{-N}\bar{\psi}_{-N}\psi_{N-1}\bar{\psi}_N\rangle$	ε_{-2N+1}	$-\mu(n,N) - \mu(n,N-1)$

[a] Subscripts on the irreducible representations ε_k would change sign if functions rather than basis vectors were subjected to symmetry operations.

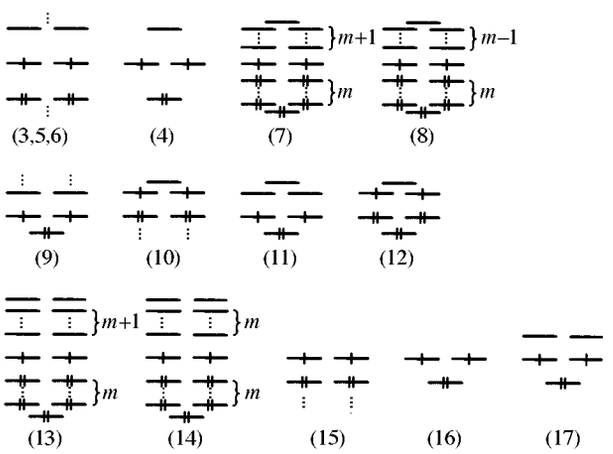

Fig. 2 The Ψ_0 configuration in the various types of $4N$-electron [n]-annulenes ($m \geqslant 1$). The numbers in parentheses are those of the Tables in which additional information is contained.

in the SO shell. Two excitations of the HO ⟶ SO type yield the configurations Ψ_{N-1}^{N} and Ψ_{-N+1}^{-N} and preserve the sense of electron circulation, as do two of the SO ⟶ LO excitations, leading to Ψ_{N}^{N+1} and Ψ_{-N}^{-N-1}. Finally, two sense-reversing HO ⟶ SO excitations, which produce Ψ_{N-1}^{-N} and Ψ_{-N+1}^{N}, and two sense-reversing SO ⟶ LO excitations, which produce Ψ_{N}^{-N-1} and Ψ_{-N}^{N+1}, are also included. The configurations and their symmetries in the C_n subgroup are listed in Table 1, which also gives the matrix elements of the z component of the magnetic dipole moment operator, which is diagonal in this basis. The magnetic moment of Ψ_0 vanishes, those of the sense-preserving configurations are small, and those of the sense-reversing configurations are large.

No electric dipole transition moments connect the lowest three configurations. Transitions from Ψ_0 are allowed only to the sense-preserving configurations, whereas transitions from Ψ_{-N}^{N} and Ψ_{N}^{-N} are allowed to two distinct pairs of sense-reversing configurations. Taking $\boldsymbol{z}$ to be the light propagation direction as well as the direction of the magnetic field, $\boldsymbol{x} + i\boldsymbol{y}$ indicates a left-handed and $\boldsymbol{x} - i\boldsymbol{y}$ a right-handed circular polarized transition that requires a photon with a z-component of angular momentum $+\hbar$ and $-\hbar$, respectively, to be absorbed.

In this configuration basis the Hamiltonian matrix is given by the expression (9), where the perturbation parameters which will be needed later are now set equal to zero, $h = h^* = s = s^* = l = l^* = 0$. The charge on the perimeter is $q = n - 4N$ and the Kronecker delta symbol δ_{iq} vanishes when $i \neq q$ and equals one when $i = q$. The resulting presence of certain matrix elements affects the final results for perimeters carrying zero, one, or two charges, and these then need to be presented separately. Also perimeters in which n and N are such that HO or LO or both are non-degenerate require a separate treatment (Fig. 2).

The energy of the degenerate configurations Ψ_{N}^{-N} and Ψ_{-N}^{N} has been subtracted along the diagonal. The non-vanishing two-electron repulsion integrals which enter the Hamiltonian matrix are those in which the overlap density due to the first electron transforms like ε_l, while that due to the second electron transforms like ε_{-l}. In the zero-differential-overlap (ZDO) approximation, the magnitude of each integral depends only on the absolute value of l and we write it as $[l]$. The integrals are positive and decrease in magnitude with increasing l from $l = 0$ to $l = n/2$ or $(n-1)/2$.

Thus integral (10) is nonzero only for r,s,t,u satisfying $s - r \equiv$

$$\iint \psi_r^*(1)\psi_s(1)(e^2/r_{12})\psi_t^*(2)\psi_u(2)\mathrm{d}\tau_1\mathrm{d}\tau_2 \qquad (10)$$

$t - u \mod n$, and is denoted by $[l]$, where $l = \min(|s-r|, n - |s-r|)$.

The quantity c is related to the one-electron energy difference of the HO and LO levels and is defined by eqn. (11). Its magnitude determines the average excitation energies and will typically be taken from experiment.

$$c = [E(\mathrm{LO}) - E(\mathrm{HO})]/2 + [1] - [2N] \qquad (11)$$

A quantity which is of crucial importance in determining the MCD signs is ΔHSL, generally defined as twice the difference between the separation ΔSH of the average one-electron energy of the SO levels [E(SO)] from that of the HO levels [E(HO)], and the separation ΔLS of the average one-electron energy of the LO levels [E(LO)] from that of the SO levels [E(SO)], eqn. (12).

$$\Delta HSL = 2(\Delta SH - \Delta LS) = 2\{|E(\mathrm{SO}) - E(\mathrm{HO})| - |E(\mathrm{LO}) - E(\mathrm{SO})|\} \qquad (12)$$

In the presently considered case of D_{nh} symmetry, the HO, SO and LO levels are all pairwise degenerate and the average energies E(HO), E(SO) and E(LO) of orbital pairs are equal to the respective orbital energies themselves.

$$
\begin{array}{llcccccccccc}
\varepsilon_0 & \Psi_0 & [2N] & \sqrt{2}s^* & \sqrt{2}s & 0 & 0 & 0 & 0 & 0 & 0 & 0 \\
\varepsilon_{2N} & \Psi_{-N}^{N} & \sqrt{2}s & 0 & [2N]\,\delta_{0q} & 0 & 0 & 0 & 0 & \sqrt{2}[2N]\,\delta_{+1q} & 0 & 0 & -\sqrt{2}[2N]\,\delta_{-1q} \\
\varepsilon_{-2N} & \Psi_{N}^{-N} & \sqrt{2}s^* & [2N]\,\delta_{0q} & 0 & 0 & 0 & 0 & 0 & 0 & -\sqrt{2}[2N]\,\delta_{-1q} & \sqrt{2}[2N]\,\delta_{+1q} & 0 \\
\varepsilon_1 & \Psi_{N}^{N+1} & 0 & 0 & 0 & c - \Delta HSL/4 + [2N+1] & -[1] & 0 & 0 & l & 0 & s^* & 0 \\
\varepsilon_1 & \Psi_{N-1}^{N} & 0 & 0 & 0 & -[1] & c + \Delta HSL/4 + [2N-1] & 0 & 0 & 0 & -h^* & 0 & -s \\
\varepsilon_{-1} & \Psi_{-N}^{-N-1} & 0 & 0 & 0 & 0 & 0 & c - \Delta HSL/4 + [2N+1] & -[1] & s & 0 & l^* & 0 \\
\varepsilon_{-1} & \Psi_{-N+1}^{-N} & 0 & 0 & 0 & 0 & 0 & -[1] & c + \Delta HSL/4 + [2N-1] & 0 & -s^* & 0 & -h \\
\varepsilon_{-2N-1} & \Psi_{N}^{-N-1} & 0 & \sqrt{2}[2N]\,\delta_{+1q} & 0 & l^* & 0 & s^* & 0 & c - \Delta HSL/4 + [1] & -[2N-1]\,\delta_{0q} & [2N]\,\delta_{+2q} + [2N+1]\,\delta_{+2q} & 0 \\
\varepsilon_{2N-1} & \Psi_{-N+1}^{N} & 0 & 0 & -\sqrt{2}[2N]\,\delta_{-1q} & 0 & -h & 0 & -s & -[2N-1]\,\delta_{0q} & c + \Delta HSL/4 + [1] & 0 & [2N]\,\delta_{-2q} + [2N-1]\,\delta_{-2q} \\
\varepsilon_{2N+1} & \Psi_{-N}^{N+1} & 0 & 0 & \sqrt{2}[2N]\,\delta_{+1q} & s & 0 & l & 0 & [2N]\,\delta_{+2q} + [2N+1]\,\delta_{+2q} & 0 & c - \Delta HSL/4 + [1] & -[2N-1]\,\delta_{0q} \\
\varepsilon_{-2N+1} & \Psi_{N-1}^{-N} & 0 & -\sqrt{2}[2N]\,\delta_{-1q} & 0 & 0 & -s^* & 0 & -h^* & 0 & [2N]\,\delta_{-2q} + [2N-1]\,\delta_{-2q} & -[2N-1]\,\delta_{0q} & c + \Delta HSL/4 + [1]
\end{array}
\qquad (9)
$$

A simple intuitive interpretation of the crucial quantity ΔHSL is to view it as a measure of the imbalance between the relative ease of excitation into and out of the half-occupied 'Fermi' level, SO. ΔHSL is negative if the former requires less energy and positive if the latter does. The alternant pairing theorem guarantees it to vanish in uncharged alternant perimeters in the present approximation, in which only the nearest-neighbor resonance integrals β_1 are kept. If needed, this approximation can be relaxed easily and the ΔHSL value can be taken from another source.

The three configurations in which the SO shell contains two electrons, Ψ_0, Ψ_N^{-N} and Ψ_{-N}^{N}, are far below the others in energy. They span the space used in the well known 3 × 3 CI model for the lowest three singlet states of biradicals.[12,15–18] The remaining eight configurations are pairwise degenerate and do not mix with the former three, except in the case of singly charged perimeters. Even then, the mixing will be weak because of the large energy gap.

State eigenfunctions

The diagonalization of the Hamiltonian matrix produces the eleven state eigenfunctions that need to be substituted into the general expressions[19] for A, B and C terms, which characterize an MCD spectrum, and for the dipole strength D, which characterizes absorption intensities.

The MCD spectrum contains a sum of contributions from all excited states. The contribution due to the transition from the ground state G into the excited state F is given by eqn. (13),

$$[\Theta]_M = -21.3458\{f_2[B(G \longrightarrow F) + C(G \longrightarrow F)/kT] + f_1 A(G \longrightarrow F)\} \quad (13)$$

where $[\Theta]_M$ is the magnetically induced molar ellipticity per unit magnetic field in deg l m^{-1} mol^{-1} G^{-1}, the line shape function f_2 is that of an absorption line and f_1 that of a derivative of an absorption line, k is Boltzmann's constant, T is absolute temperature, and $A(G \longrightarrow F)$, $B(G \longrightarrow F)$ and $C(G \longrightarrow F)$ are the Faraday parameters of the $G \longrightarrow F$ transition. A is in units of $D^2\beta_e$ and B and C/kT are in units of $D^2\beta_e/cm^{-1}$. In a molecule with a non-degenerate ground state, $C(G \longrightarrow F)$ vanishes for all F. If the excited state F also is non-degenerate, $A(G \longrightarrow F)$ vanishes as well. Note that a negative B term corresponds to a positive peak in the MCD spectrum.

The values of the A, B and C terms are usually obtained from the measured spectra using the method of moments. For an isotropic solution,

$$A = 33.53^{-1} \int d\tilde{\nu}\,(\tilde{\nu} - \tilde{\nu}_0)[\Theta]_M/\tilde{\nu} \quad (14)$$
$$B + C/kT = 33.53^{-1} \int d\tilde{\nu}[\Theta]_M/\tilde{\nu}$$

where $\tilde{\nu}$ is wavenumber and $\tilde{\nu}_0$ is the center of the absorption band. The integration is over the region of the band due to the $G \longrightarrow F$ transition.

When vibrational fine structure is ignored, the following expressions result from the use of first-order perturbation theory for the effect of the magnetic field:

$$A(G \longrightarrow F) = (1/2g) \sum_{\gamma\alpha} (\langle F_\alpha|\hat{\mathcal{M}}|F_\alpha\rangle - \langle G_\gamma|\hat{\mathcal{M}}|G_\gamma\rangle) \cdot Im(\langle G_\gamma|\hat{\boldsymbol{M}}|F_\alpha\rangle \times \langle F_\alpha|\hat{\boldsymbol{M}}|G_\gamma\rangle) \quad (15)$$

$$B(G \longrightarrow F) = (1/g) \sum_{\gamma\alpha} Im \left\{ \sum_{\substack{K\kappa \\ K \neq F}} \langle F_\alpha|\hat{\mathcal{M}}|K_\kappa\rangle \cdot \langle G_\gamma|\hat{\boldsymbol{M}}|F_\alpha\rangle \times \langle K_\kappa|\hat{\boldsymbol{M}}|G_\gamma\rangle / [W(K) - W(F)] + \sum_{\substack{K\kappa \\ K \neq G}} \langle K_\kappa|\hat{\mathcal{M}}|G_\gamma\rangle \cdot \langle G_\gamma|\hat{\boldsymbol{M}}|F_\alpha\rangle \times \langle F_\alpha|\hat{\boldsymbol{M}}|K_\kappa\rangle / [W(K) - W(G)] \right\} \quad (16)$$

$$C(G \longrightarrow F) = (1/2g) \sum_{\gamma\alpha} \langle G_\alpha|\hat{\mathcal{M}}|G_\gamma\rangle \cdot Im(\langle G_\gamma|\hat{\boldsymbol{M}}|F_\alpha\rangle \times \langle F_\alpha|\hat{\boldsymbol{M}}|G_\gamma\rangle) \quad (17)$$

where the Greek subscripts identify the components of the possibly degenerate states G, K and F, and g is the degeneracy of the ground state. The summation over K runs over all electronic states. *Im* stands for 'imaginary part of', $\hat{\boldsymbol{M}} = \Sigma_i \hat{\boldsymbol{m}}_i$ is the total electric dipole moment operator and $\hat{\mathcal{M}} = \Sigma_i \hat{\boldsymbol{\mu}}_i$ is the total magnetic dipole moment operator. $W(I)$ denotes the energy of the state I. The wavefunctions $|G\rangle$, $|K\rangle$ and $|F\rangle$ are those in the absence of magnetic field.

The dipole strength D is defined by eqn. (18).

$$D(G \longrightarrow F) = (1/g) \sum_{\gamma\alpha} |\langle F_\alpha|\hat{\boldsymbol{M}}|G_\gamma\rangle|^2 \quad (18)$$

In the following, we consider first the idealized case of singlet states of $4N$-electron [n]annulenes at D_{nh} symmetry, although in reality measurements on the lowest singlet state cannot be done at this geometry because of pseudo-Jahn–Teller distortions (in uncharged annulenes) or Jahn–Teller distortions (in charged annulenes). However, the results for D_{nh} symmetry will serve as the starting points for the discussion of perturbations which produce observable systems, either weakly perturbed antiaromatic ones (Part 1) or strongly perturbed unaromatic ones (Parts 2 and 3).

Some statements about the results are general but quite a few differences exist between the charged and the uncharged perimeters, which will therefore be discussed separately. Table 2 lists all the special cases that need to be treated separately in view of the coincidence of some irreducible representations of the C_n group that are distinct in the general case.

Four abbreviations that will be found useful in the following are given in eqn. (19). The magnetic moments $\mu_\pm$, relevant

$$\Delta^{-1}(X,Y) \equiv [W(X) - W(Y)]^{-1}; m_\pm \equiv m(n,2N+1) \pm m(n,2N-1); \mu \equiv \mu(n,N); \mu_\pm \equiv \mu(n,N+1) \pm \mu(n,N-1) \quad (19)$$

for $4N$-electron perimeters, should not be confused with the related but differently defined magnetic moments $\mu^\pm$ defined earlier[8] for $(4N + 2)$-electron perimeters.

3. Magnetic circular dichroism of uncharged antiaromatic D_{nh} $4N$-electron [n]annulenes ($4N = n$)

3.1 General ($n > 4$)

All eleven configurations need to be considered. For uncharged D_{nh} symmetry [n]annulenes the representations ε_{2N} and ε_{-2N} coincide and are labeled b in the C_n symmetry group. Thus Ψ_{-N}^{N} and Ψ_N^{-N} are coupled through a matrix element of the two-electron part of the Hamiltonian, equal to $[2N]$. The resulting in-phase combination $B^{(+)} = (\Psi_{-N}^{N} + \Psi_N^{-N})/\sqrt{2}$ is destabilized by $[2N]$ and together with $A = \Psi_0$ forms the first excited accidentally doubly degenerate singlet state. The exact degeneracy is lifted in more extensive CI calculations.[18] The character and the properties of the two components are however not changed much relative to the simple model, since the splitting is not due to their direct mutual interaction.

The out-of-phase combination $B^{(-)} = (\Psi_{-N}^{N} - \Psi_N^{-N})/\sqrt{2}$ is stabilized by $[2N]$ and becomes the lowest singlet state G, degenerate with the lowest triplet state. The ambiguity concerning the nature of the true ground state has been resolved in favor of the singlet state by calculations which include a larger configuration basis that comprises all excitations within the π levels or even include correlation for σ electrons.[18] Thus, it is reasonable to take the out-of-phase combination $B^{(-)} = (\Psi_{-N}^{N} - \Psi_N^{-N})/$

Table 2 Classes of antiaromatic 4*N*-electron [*n*]annulenes

N	*n*	Example	Degeneracy HO	SO	LO	Special symmetry properties
1	3	$C_3H_3^-$	1	2	0	
1	4	C_4H_4	1	2	1	
1	5	$C_5H_5^+$	1	2	2	$\varepsilon_{2N-1} = \varepsilon_1$ $\varepsilon_{2N} = \varepsilon_{-2N-1}$
1	6	$C_6H_6^{2+}$	1	2	2	$\varepsilon_{2N-1} = \varepsilon_1$ $\varepsilon_{2N+1} = \varepsilon_{-2N-1}$
1	7	$C_7H_7^{3+}$	1	2	2	$\varepsilon_{2N-1} = \varepsilon_1$
2	6	$C_6H_6^{2-}$	2	2	1	$\varepsilon_{2N+1} = \varepsilon_{-1}$ $\varepsilon_{2N-1} = \varepsilon_{-2N+1}$
>1	$2N + 2$	$C_8H_8^{4-}$	2	2	1	$\varepsilon_{2N+1} = \varepsilon_{-1}$
>1	$2N + 1$	$C_7H_7^{5-}$	2	2	0	$\varepsilon_{2N} = \varepsilon_{-1}$
>1	$4N + 2$	$C_{10}H_{10}^{2+}$	2	2	2	$\varepsilon_{2N+1} = \varepsilon_{-2N-1}$
>1	$4N - 2$	$C_{10}H_{10}^{2-}$	2	2	2	$\varepsilon_{2N-1} = \varepsilon_{-2N+1}$
>1	$4N + 1$	$C_9H_9^+$	2	2	2	$\varepsilon_{2N+1} = \varepsilon_{-2N}$
>1	$4N - 1$	$C_7H_7^-$	2	2	2	$\varepsilon_{2N-1} = \varepsilon_{-2N}$
>1	$4N$	C_8H_8	2	2	2	$\varepsilon_{2N+1} = \varepsilon_{-2N+1}$
>2	$2N + 1 < n < 4N - 2$ or $n > 4N + 2$	$C_{11}H_{11}^{3+}$, $C_{11}H_{11}^{5-}$	2	2	2	

Table 3 4*N*-Electron [4*N*]annulenes ($N > 1$)[a]

State	Energy	D[b]	$\mathcal{M}$[b,c]	B[b]
$B_{1g}^{(-)}$	$-[2N]$	—	0	—
$B_{2g}^{(+)}$	$[2N]$	0	0	0
$A_{1g}^{(-)}$	$[2N]$	0	0	0
$E_{1u}^{(-)}$	$c - [1] + [2N - 1]$	0	$\mu_-/2$	0
$E_{2N+1,u}^{(-)}$	$c + [1] - [2N - 1]$	m_-^2	$\mu_-/2$	$-2[\Delta^{-1}(B_{2g}^{(+)},B_{1g}^{(-)})\mu + \Delta^{-1}(E_{2N+1,u}^{(+)},E_{2N+1,u}^{(-)})(\mu_+ + 2\mu)/4]m_+m_-$
$E_{2N+1,u}^{(+)}$	$c + [1] + [2N - 1]$	m_+^2	$\mu_-/2$	$-2[\Delta^{-1}(B_{2g}^{(+)},B_{1g}^{(-)})\mu - \Delta^{-1}(E_{2N+1,u}^{(+)},E_{2N+1,u}^{(-)})(\mu_+ + 2\mu)/4]m_+m_-$
$E_{1u}^{(+)}$	$c + [1] + [2N - 1]$	0	$\mu_-/2$	0

[a] $m_+ \equiv m(n,2N+1) + m(n,2N-1)$, $m_- \equiv m(n,2N+1) - m(n,2N-1)$, $\mu_+ \equiv \mu(n,N+1) + \mu(n,N-1)$, $\mu_- \equiv \mu(n,N+1) - \mu(n,N-1)$, $\mu \equiv \mu(n,N)$, $\Delta^{-1}(X,Y) \equiv [W(X) - W(Y)]^{-1}$. [b] Spectroscopic characteristics of transitions from the $B_{1g}^{(-)}$ state. [c] State magnetic moment. For allowed excited states, equal to $-2(A + C)/D$. If $D = 0$, the sign of $\mathcal{M}$ is ambiguous.

$\sqrt{2}$ as the ground state G of uncharged unperturbed D_{nh} annulenes.[20]

The remainder of the Hamiltonian matrix (9) simplifies since for uncharged alternant perimeters we have $\Delta HSL = 0$ by the alternant pairing theorem. The sense-preserving ε_1 configurations Ψ_N^{N+1} and Ψ_{N-1}^N interact through the two-electron part of the Hamiltonian, and the two sense-preserving ε_{-1} configurations related to them by complex conjugation do likewise, to yield ultimately two doubly degenerate excited states of E_1 ($\equiv\varepsilon_1,\varepsilon_{-1}$) symmetry, $E_1^{(-)}$ and $E_1^{(+)}$ (Table 3). In the C_{4N} symmetry groups the representations ε_{2N-1} and $\varepsilon_{-(2N+1)}$ coincide, as do their complex conjugates $\varepsilon_{-(2N-1)}$ and ε_{2N+1}. Configurations that belong to these irreducible representations are coupled through the two-electron part of the Hamiltonian and give rise to two doubly degenerate states of symmetry E_{2N+1} [$\equiv\varepsilon_{2N+1},\varepsilon_{-(2N+1)}$], equal to E_{2N-1} [$\equiv\varepsilon_{2N-1}$, $\varepsilon_{-(2N-1)}$]. These shall be labeled $E_{2N+1}^{(-)}$ and $E_{2N+1}^{(+)}$ (Table 3).

The energies of the electronic states increase in the order $G \equiv B^{(-)}$, $B^{(+)}$, $A^{(-)}$, $E_1^{(-)}$, $E_{2N+1}^{(-)}$, $E_{2N+1}^{(+)}$ and $E_1^{(+)}$, with the $B^{(+)}$ and $A^{(-)}$ as well as the $E_{2N+1}^{(+)}$ and $E_1^{(-)}$ states forming accidentally degenerate pairs within the ZDO approximation. The labels (+) and (−) are related to the in-phase and out-of-phase mixing of complex configurations and indicate whether the contributions to the transition moments from the ground state add (+) or cancel (−). In the full D_{nh} symmetry group, the labels become $G \equiv B_{1g}^{(-)}$ for the ground state, and $B_{2g}^{(+)}$, $A_{1g}^{(-)}$, $E_{1u}^{(-)}$, $E_{2N+1,u}^{(-)}$, $E_{2N+1,u}^{(+)}$ and $E_{1u}^{(+)}$ for the excited states. The energies and other properties of these states are summarized in Table 3. For uncharged perimeters, which are alternant, the (+) and (−) symbols indicate the parity of a state in the sense of Pariser's alternant pairing, in a way familiar from aromatic systems.[21–24]

Only $G \longrightarrow E_{2N+1}^{(-)}$ and $G \longrightarrow E_{2N+1}^{(+)}$ are allowed by symmetry as electric-dipole transitions. As indicated by the (−) superscript, the dipole strength for the former vanishes within the model due to a cancellation of the configuration transition moments involved, $m(n,2N+1) = m(n,2N-1)$, as do the B

terms of both. Thus, the only intense transition that should be observed in ordinary absorption or MCD spectra is $G \longrightarrow E^{(+)}_{2N+1}$, which has a non-vanishing A term.

The magnetic moments of the $B^{(-)}$, $A^{(-)}$ and $B^{(+)}$ states vanish. Those of the other excited states are identical in magnitude and small, as they are given by half the difference of the HO and LO orbital magnetic moments, $\mu_-/2$. Within the model, μ_- vanishes if only the nearest-neighbor resonance integrals β_1 are kept. Thus, the A terms of all uncharged $4N$-electron annulenes vanish exactly in the perfect alternant pairing approximation, as expected from a general theorem.[25] In order to obtain sign predictions, it is necessary to go beyond this approximation in the evaluation of the difference of the HO and LO orbital magnetic moments, μ_-. We then find that it is proportional to the normally neglected next-nearest-neighbor resonance integrals. This, then, is the excuse for keeping these integrals in the evaluation of magnetic moment matrix elements, even though the resonance integrals between next-nearest AOs are not kept. In this respect the μ_- moments are very similar to the μ^- magnetic moment defined for uncharged aromatic annulenes.[8] Both would reverse their signs (incorrectly) if one failed to perform a Löwdin orthogonalization explicitly before computing the matrix elements of the magnetic dipole moment operator in a ZDO-type calculation.[8,26]

Only the symmetry-allowed transitions to the $E^{(+)}_{2N+1}$ and $E^{(-)}_{2N+1}$ states can show non-vanishing B terms. Within the perfect alternant pairing scheme, the resultant B terms are calculated to be zero since they are proportional to the difference m_- which vanishes within the model due to alternant pairing. This is again in keeping with the general theorem.[25]

The fact that $m(n,2N+1)$ is equal to $m(n,2N-1)$, causing m_- to vanish, is a consequence of the neglect of third and higher powers of overlap in the explicit Löwdin orthogonalization of the AO basis used to derive eqn. (2). If the orthogonalization is done exactly, m_- is calculated to be very slightly different from zero. Insofar as the consequences of this are detectable at all, they will result in a non-vanishing intensity and a positive A term for the transition $G \longrightarrow E^{(-)}_{2N+1}$, as well as nonvanishing B terms for the two symmetry-allowed transitions, $G \longrightarrow E^{(-)}_{2N+1}$ and $G \longrightarrow E^{(+)}_{2N+1}$. The B terms contain contributions from the coupling of the $B^{(+)}_{2g}$ state with the ground state and from the mutual magnetic mixing of the two E_{2N+1} states. The former contribution has the sign of m_- and is identical for both B terms, whereas the latter contribution has opposite signs for $G \longrightarrow E^{(-)}_{2N+1}$ and for $G \longrightarrow E^{(+)}_{2N+1}$. Thus, the B term expected for the $E^{(-)}_{2N+1}$ state has inevitably the sign of m_-. The resulting sign of the B term of the higher-energy $E^{(+)}_{2N+1}$ state depends on the relative magnitudes of the state energy differences. In general, it will be very small and hard to detect next to the positive A term. It should be reemphasized that all of the effects due to the minute difference between $m(n,2N+1)$ and $m(n,2N-1)$ should be quite small and are likely to be negligible relative to vibronic effects which we do not consider here at all.

3.2 D_{4h} [4]Annulene ($n = 4N = 4$)

Square cyclobutadiene is one of the special cases listed in Table 2. The HO and LO levels are not degenerate (a and b, respectively, in the C_n group), leaving only seven of the general eleven configurations (Table 4). The states $B^{(-)} \equiv B^{(-)}_{1g}$, $B^{(+)} \equiv B^{(+)}_{2g}$ and $A^{(-)} \equiv A^{(-)}_{1g}$ states are not affected, but now only two doubly degenerate states, $E^{(-)}_1 \equiv E^{(-)}_{2N+1} \equiv E^{(-)}_{1u}$ and $E^{(+)}_1 \equiv E^{(+)}_{2N+1} \equiv E^{(+)}_{1u}$, arise. Transitions into both are symmetry allowed, and the $G \longrightarrow E^{(+)}_1$ transition should be strong, but its B term vanishes through second order in overlap, as do the dipole strength and the B term for the $G \longrightarrow E^{(-)}_1$ transition. The magnetic moments and A terms of the excited states vanish since the orbital moments for the non-degenerate HO and LO levels are zero.

When third and higher powers of overlap are not neglected, a very small dipole strength for the $G \longrightarrow E^{(-)}_1$ transition and small non-zero B terms for both symmetry allowed transitions result, as they did in the general case. Now both B terms are negative since m_- is positive and the contribution of the mixing of the $B^{(+)}$ state into the ground state dominates in the previously ambiguous case of the higher energy transition.

Table 4 4-Electron [4]annulene[a]

State	Energy	D	$\mathcal{M}$	B
$B^{(-)}_{1g}$	$-[2]$	—	0	—
$B^{(+)}_{2g}$	[2]	0	0	0
$A^{(-)}_{1g}$	[2]	0	0	0
$E^{(-)}_{1u}$	c	m^2_-	0	$-2\mu[\Delta^{-1}(B^{(+)}_{2g},B^{(-)}_{1g}) + \Delta^{-1}(E^{(+)}_{1u},E^{(-)}_{1u})/2]m_+m_-$
$E^{(+)}_{1u}$	$c + 2[1]$	m^2_+	0	$-2\mu[\Delta^{-1}(B^{(+)}_{2g},B^{(-)}_{1g}) - \Delta^{-1}(E^{(+)}_{1u},E^{(-)}_{1u})/2]m_+m_-$

[a] See footnotes in Table 3.

4. Magnetic circular dichroism of charged D_{nh} antiaromatic $4N$-electron [n]annulenes ($4N \neq n$)

4.1 General ($|4N - n| > 2$)

All eleven configurations again need to be considered. However, now the C_n group representations ε_{2N+1} and $\varepsilon_{-(2N-1)}$ are distinct, as are ε_{2N-1} and $\varepsilon_{-(2N+1)}$. The configurations of these symmetries no longer interact, as they did for uncharged perimeters.

The lowest singlet is then doubly degenerate, with the components ε_{2N} and ε_{-2N}. The third low-energy singlet wave function is of A symmetry and lies higher by $[2N]$. The lowest triplet lies lower by the same amount. In several known systems of this kind the triplet is indeed the ground state in reality, but this is not always so.[18] As before,[20] the integral $[2N]$ is equal to $K'_{AB} + K_{AB}$ when expressed in integrals over the localized orbitals Ψ_A and Ψ_B, but now symmetry enforces the equality $K'_{AB} = K_{AB}$, whereas for the uncharged antiaromatic annulenes K_{AB} vanished in the ZDO approximation. In both instances, the splitting between the lowest two singlet states is $2K'$, but now, the lowest singlet E_{2N} is degenerate.[27]

In the following, we present results for the spectral properties of the E_{2N} state predicted from the simple model as the ground state at the ideal D_{nh} geometry, since this acts as the parent of the ground state of the perturbed systems of actual interest. It is believed[18] that in some real systems the non-degenerate A state actually is the ground state instead. Results for its spectra could be obtained similarly but we shall only illustrate them on an example for which experimental evidence suggests that they are needed.

Turning attention to the lower right blocks of the 11×11 Hamiltonian matrix (9), we note that only the ε_1 symmetry configurations and their complex conjugates interact to give $E^{(-)}_1$ and $E^{(+)}_1$ states, whereas the E_{2N+1} and E_{2N-1} states are represented by the initial configurations alone (Tables 5 and 6). The ordering of the E_{2N+1} and E_{2N-1} states as well as the relative weight of the two configurations entering the $E^{(-)}_1$ and $E^{(+)}_1$ states are determined primarily by the magnitude and especially the sign of the quantity ΔHSL, defined in eqn. (12). For positively charged perimeters (Table 5), excitation into the 'Fermi' (SO) level takes less energy than excitation out of it, and $\Delta HSL < 0$. The E_{2N-1} state lies below E_{2N+1}, and the configurations describing the HO $\longrightarrow$ SO excitations dominate the $E^{(+)}_1$ state. For negatively charged perimeters (Table 6), excitation out of the 'Fermi' level takes less energy, and $\Delta HSL > 0$. The E_{2N-1} state lies above E_{2N+1} and the SO $\longrightarrow$ LO excited configurations dominate the $E^{(-)}_1$ state.

Table 5 $4N$-Electron [n]annulene cations ($n > 4N + 2$ and $N > 1$)[a,b]

State[e]	Energy	D^d	$\mathcal{M}^{c,d}$	B^d	C^d
$E_{2N,g}$	0	—	2μ	—	—
A_{1g}	$[2N]$	0	0	0	0
$E_{1u}^{(+)}$	$c + [2N + 1] + [1]/\tan\beta - \Delta HSL/4$	0	$\mu_-/2 - (\mu_+/2 - \mu)\cos 2\beta$	0	0
$E_{2N-1,u}$	$c + [1] + \Delta HSL/4$	$2m^2(n,2N-1)$	$-[\mu(n,N) + \mu(n,N-1)]$	0	$2\mu m^2(n,2N-1)$
$E_{2N+1,u}$	$c + [1] - \Delta HSL/4$	$2m^2(n,2N+1)$	$+[\mu(n,N) + \mu(n,N+1)]$	0	$-2\mu m^2(n,2N+1)$
$E_{1u}^{(-)}$	$c + [2N + 1] - [1]\tan\beta - \Delta HSL/4$	0	$\mu_-/2 + (\mu_+/2 - \mu)\cos 2\beta$	0	0

[a] See footnote *a* in Table 3. [b] $\beta = (1/2)\tan^{-1}\{2[1]/(\Delta HSL/2 + [2N-1] - [2N+1])\}$. [c] See footnote *c* in Table 3. [d] Spectroscopic characteristics of transitions from the $E_{2N,g}$ state. [e] Symbol u and g apply only if n is even.

Table 6 $4N$-Electron [n]annulene anions {$4N > n + 2$ and $N \leqslant (n-1)/2$ [n odd] or $N \leqslant (n-2)/2$ [n even]}[a,b]

State[e]	Energy	D^d	$\mathcal{M}^{c,d}$	B^d	C^d
$E_{2N,g}$	0	—	2μ	—	—
A_{1g}	$[2N]$	0	0	0	0
$E_{1u}^{(-)}$	$c + [2N + 1] - [1]\tan\beta - \Delta HSL/4$	0	$\mu_-/2 + (\mu_+/2 - \mu)\cos 2\beta$	0	0
$E_{2N+1,u}$	$c + [1] - \Delta HSL/4$	$2m^2(n,2N+1)$	$\mu(n,N) + \mu(n,N+1)$	0	$-2\mu m^2(n,2N+1)$
$E_{2N-1,u}$	$c + [1] + \Delta HSL/4$	$2m^2(n,2N-1)$	$-\mu(n,N) - \mu(n,N-1)$	0	$2\mu m^2(n,2N-1)$
$E_{1u}^{(+)}$	$c + [2N + 1] + [1]/\tan\beta - \Delta HSL/4$	0	$\mu_-/2 - (\mu_+/2 - \mu)\cos 2\beta$	0	0

[a] See footnote *a* in Table 3. [b] See footnote *b* in Table 5. [c] See footnote *c* in Table 3. [d] Spectroscopic characteristics of transitions from the $E_{2N,g}$ state. [e] Symbols u and g apply only if n is even.

Only transitions from the ground state to the E_{2N+1} and E_{2N-1} states are allowed. Their relative intensity depends on the ratio $m(n,2N+1)/m(n,2N-1)$, and this is very close to unity [eqn. (6)]. The A terms are determined by the differences $\mu(n,N+1) - \mu(n,N)$ for the E_{2N+1} state and $\mu(n,N) - \mu(n,N-1)$ for the E_{2N-1} state. These differences are familiar from work with $(4N + 2)$-electron [n]annulenes, the former being equal to $\mu^-(n,N)$ and the latter to $\mu^-(n,N-1)$.[8] The former is positive for positively charged perimeters and negative for negatively charged ones. The latter is negative except for highly charged anionic perimeters. Thus, the signs of both A terms are positive for cations, but they differ for anions, with $A(G \longrightarrow E_{2N+1}) < 0$ and $A(G \longrightarrow E_{2N-1}) > 0$, unless their charge is high enough to make both terms negative. The B terms vanish. The C terms are always positive for the $G \longrightarrow E_{2N+1}$ and negative for the $G \longrightarrow E_{2N-1}$ transition.

Since the charged perimeters are either non-alternant (n odd) or alternant but not self-paired (n even), their states cannot be labeled by the eigenvalues of the pairing operator.[21–24] We use the labels (+) and (−) in a less rigorous sense to indicate addition or cancellation of the contributions to the transition moment from the ground state that are provided by the configurations that enter into the excited state, and in some cases, merely to distinguish states of equal symmetry.

4.2 4*N*-Electron [4*N* + 2]annulenes (*n* > 6)

In these dications (Table 7) the irreducible representations ε_{2N+1} and $\varepsilon_{-(2N+1)}$ of the C_{4N+2} group coincide and are labeled b. Two non-degenerate states of B symmetry are found instead of the usual E_{2N+1} state. The properties of the E_{2N-1} states are preserved and the predictions of the previous discussion hold. The dipole strength of the split state is distributed equally between the two new B states. Their mutual magnetic mixing causes quite large B terms for both, positive for the lower and negative for the upper state. The C terms of both are positive.

Table 7 also lists the spectroscopic properties of the A_{1g} singlet state since this appears to be the ground state of some systems derived from the analogous dianion perimeters (see section 4.3).[28] Only the transitions into the lower $E_1^{(+)}$ and upper $E_1^{(-)}$ states have non-vanishing dipole strengths. The former has a small and the latter a large positive A term.

4.3 4*N*-Electron [4*N* − 2]annulenes (*n* > 6)

In these dianions (Table 8) the irreducible representations ε_{2N-1} and $\varepsilon_{-(2N-1)}$ of the C_{4N+2} group coincide, and two non-degenerate states of B symmetry are found instead of the usual E_{2N-1} state. The usual general results of Section 4.1 hold for the E_{2N+1} state. The two B states share equally the dipole strength of the parent E_{2N-1} state. The lower one has a negative and the upper one a positive B term. Their C terms are negative.

Since certain real molecules derived from perimeters of this kind appear to have the A_{1g} singlet as the ground state,[28] we have also listed in Table 8 the spectroscopic properties for excitation out of this state. Only the transitions into the $E_1^{(-)}$ and $E_1^{(+)}$ states have non-vanishing dipole strengths. The former has a small and the latter a large negative A term. The B term of the $A_{1g} \longrightarrow E_1^{(-)}$ transition is negative, that of the $A_{1g} \longrightarrow E_1^{(+)}$ transition is positive.

In the perfect alternant pairing approximation, in which only the AO matrix elements of $\hat{\boldsymbol{\mu}}$ between nearest neighbors are kept, the MCD spectra of the dication and the dianion of an [n]annulene are mirror images of each other, as required by a general theorem.[25]

4.4 4-Electron [*n*]annulenes (*n* > 6)

In these cations (Table 9), the HO level is non-degenerate and the $\varepsilon_{-(2N-1)}$ configurations are absent. Three doubly degenerate excited states are obtained in addition to the ground state (E_2) and the first excited state (A). They are $E_1^{(-)}$, E_3 ($\equiv E_{2N+1}$) and $E_1^{(+)}$. The two components of the E_3 state are Ψ_{-N}^{N+1} and Ψ_{N}^{-N-1}.

The transition $G \longrightarrow E_3$ is allowed and shows the usual A

Table 7 $4N$-Electron [$4N + 2$]annulene dications ($N > 1$) [a,b]

State	Energy	D [d]	$\mathscr{M}$ [c,d]	B [d]	C [d]	D [e]	B [e]
$E_{2N,g}$	0	—	2μ	—	—	0	0
A_{1g}	$[2N]$	0	0	0	0	—	—
$E_{1u}^{(+)}$	$c + [1]/\tan\beta + [2N + 1] - \Delta HSL/4$	0	$\mu_-/2 + (\mu - \mu_+/2) \times \cos 2\beta$	0	0	$[m^2{}_+ - 2m_+m_- \cos 2\beta + m^2{}_- + (m^2{}_+ - m^2{}_-) \sin 2\beta]/2$	$-\Delta^{-1}(E_{1u}^{(+)},E_{1u}^{(-)})(2\mu - \mu_+) \times \cos\beta \sin\beta\,[2m_+m_- \sin 2\beta + (m^2{}_+ - m^2{}_-) \cos 2\beta]/2$
$B_{1u}^{(-)}$	$c + [1] - [2N] - \Delta HSL/4 - [2N + 1]$	$m^2(n,2N + 1)$	0	$-\Delta^{-1}(B_{2u}^{(+)},B_{1u}^{(-)}) \times m^2(n,2N + 1) \times [\mu + (\mu_+ + \mu_-)/2]$	$-\mu m^2(n,2N + 1)$	0	0
$E_{2N-1,u}$	$c + [1] + \Delta HSL/4$	$2m^2(n,2N - 1)$	$-[\mu + (\mu_+ - \mu_-)/2]$	0	$2\mu m^2(n,2N - 1)$	0	0
$E_{1u}^{(-)}$	$c - [1] \tan\beta - \Delta HSL/4 + [2N + 1]$	0	$\mu_-/2 - (\mu - \mu_+/2) \times \cos 2\beta$	0	0	$[m^2{}_+ + 2m_+m_- \cos 2\beta + m^2{}_- - (m^2{}_+ - m^2{}_-) \sin 2\beta]/2$	$\Delta^{-1}(E_{1u}^{(+)},E_{1u}^{(-)})(2\mu - \mu_+) \times \cos\beta \sin\beta\,[2m_+m_- \sin 2\beta + (m^2{}_+ - m^2{}_-) \cos 2\beta]/2$
$B_{2u}^{(+)}$	$c + [1] + [2N] - \Delta HSL/4 + [2N + 1]$	$m^2(n,2N + 1)$	0	$\Delta^{-1}(B_{2u}^{(+)},B_{1u}^{(-)}) \times m^2(n,2N + 1) \times [\mu + (\mu_+ + \mu_-)/2]$	$-\mu m^2(n,2N + 1)$	0	0

[a] See footnote *a* in Table 3. [b] See footnote *b* in Table 5. [c] See footnote *c* in Table 3. [d] Spectroscopic characteristics of transitions from the $E_{2N,g}$ state. [e] Spectroscopic characteristics of transitions from the A_{1g} state.

Table 8 $4N$-Electron [$4N - 2$]annulene dianions ($N > 2$) [a,b]

State	Energy	D [d]	$\mathscr{M}$ [c,d]	B [d]	D [e]	B [e]
$E_{2N,g}$	0	—	2μ	—	0	0
A_{1g}	$[2N]$	0	0	0	—	—
$E_{1u}^{(-)}$	$c - [1] \tan\beta - \Delta HSL/4 + [2N + 1]$	0	$\mu_-/2 - (\mu - \mu_+/2) \cos 2\beta$	0	$[m^2_+ + 2m_+m_- \cos 2\beta + m^2_- - (m^2_+ - m^2_-) \sin 2\beta]/2$	$\Delta^{-1}(E_{1u}^{(+)},E_{1u}^{(-)})(2\mu - \mu_+) \times \sin 2\beta\,[2m_+m_- \sin 2\beta + (m^2_+ - m^2_-) \cos 2\beta]/4$
$B_{1u}^{(-)}$	$c + [1] - [2N] + \Delta HSL/4 - [2N - 1]$	$m^2(n,2N - 1)$	0	$\Delta^{-1}(B_{2u}^{(+)},B_{1u}^{(-)})m^2(n,2N - 1) \times [\mu + (\mu_+ - \mu_-)/2]$	0	0
$E_{2N+1,u}$	$c + [1] - \Delta HSL/4$	$2m^2(n,2N + 1)$	$\mu + (\mu_+ + \mu_-)/2$	0	0	0
$E_{1u}^{(+)}$	$c + [1]/\tan\beta - \Delta HSL/4 + [2N + 1]$	0	$\mu_-/2 + (\mu - \mu_+/2) \cos 2\beta$	0	$[m^2_+ - 2m_+m_- \cos 2\beta + m^2_- + (m^2_+ - m^2_-) \sin 2\beta]/2$	$-\Delta^{-1}(E_{1u}^{(+)},E_{1u}^{(-)})(2\mu - \mu_+) \times \sin 2\beta\,[2m_+m_- \sin 2\beta + (m^2_+ - m^2_-) \cos 2\beta]/4$
$B_{2u}^{(+)}$	$c + [1] + [2N] + \Delta HSL/4 + [2N - 1]$	$m^2(n,2N - 1)$	0	$-\Delta^{-1}(B_{2u}^{(+)},B_{1u}^{(-)})m^2(n,2N - 1) \times [\mu + (\mu_+ - \mu_-)/2]$	0	0

[a] See footnote *a* in Table 3. [b] See footnote *b* in Table 5. [c] See footnote *c* in Table 3. [d] Spectroscopic characteristics of transitions from the $E_{2N,g}$ state. [e] Spectroscopic characteristics of transitions from the A_{1g} state.

Table 9 4-Electron [*n*]annulene cations ($n > 6$)[a,b]

State[e]	Energy	D[d]	$\mathscr{M}$[c,d]	B[d]	C[d]
E_{2g}	0	—	2μ	—	—
A_{1g}	[2]	0	0	0	0
$E_{1u}^{(+)}$	$c + [1]/\tan\beta - \Delta HSL/4 + [3]$	$2m^2(n,1)\cos^2\beta$	$-\mu\cos 2\beta - \mu(n,2)\sin^2\beta$	$+\Delta^{-1}(E_{1u}^{(-)},E_{1u}^{(+)}) \times [2\mu - \mu(n,2)] \times \sin^2 2\beta m^2(n,1)/2$	$2\mu\cos^2\beta m^2(n,1)$
E_{3u}	$c + [1] - \Delta HSL/4$	$2m^2(n,3)$	$\mu + \mu(n,2)$	0	$-2\mu m^2(n,3)$
$E_{1u}^{(-)}$	$c - [1]\tan\beta - \Delta HSL/4 + [3]$	$2m^2(n,1)\sin^2\beta$	$\mu\cos 2\beta - \mu(n,2)\cos^2\beta$	$-\Delta^{-1}(E_{1u}^{(-)},E_{1u}^{(+)}) \times [2\mu - \mu(n,2)] \times \sin^2 2\beta m^2(n,1)/2$	$2\mu\sin^2\beta m^2(n,1)$

[a] See footnote *a* in Table 3. [b] $\beta = (1/2)\tan^{-1}\{2[1]/(\Delta HSL/2 + [1] - [3])\}$. [c] See footnote *c* in Table 3. [d] Spectroscopic characteristics of transitions from the E_{2g} state. [e] Symbols u and g apply only if *n* is even.

Table 10 $4N$-Electron $[2N + 2]$annulene anions ($n > 6$)[a,b]

State	Energy	D[d]	$\mathscr{M}$[c,d]	B[d]	C[d]
E_{2g}	0	—	2μ	—	—
A_{1g}	[2]	0	0	0	0
$E_{1u}^{(-)}$	$c - [1]\tan\beta - \Delta HSL/4 + [2N + 1]$	$2m^2(n,2N + 1)\cos^2\beta$	$\mu\cos 2\beta + \mu(n,N - 1)\sin^2\beta$	$-\Delta^{-1}(E_{1u}^{(+)},E_{1u}^{(-)}) \times [2\mu - \mu(n,N - 1)] \times \sin^2 2\beta m^2(n,2N + 1)/2$	$-2\mu\cos^2\beta m^2(n,2N + 1)$
E_{3u}	$c + \Delta HSL/4 + [1]$	$2m^2(n,2N - 1)$	$-[\mu + \mu(n,N - 1)]$	0	$2\mu m^2(n,2N - 1)$
$E_{1u}^{(+)}$	$c + [1]/\tan\beta - \Delta HSL/4 + [2N + 1]$	$2m^2(n,2N + 1)\sin^2\beta$	$-\mu\cos 2\beta + \mu(n,N - 1)\cos^2\beta$	$\Delta^{-1}(E_{1u}^{(+)},E_{1u}^{(-)}) \times [2\mu - \mu(n,N - 1)] \times \sin^2 2\beta m^2(n,2N + 1)/2$	$-2\mu\sin^2\beta m^2(n,2N + 1)$

[a] See footnote *a* in Table 3. [b] $\beta = (1/2)\tan^{-1}\{2[1]/(\Delta HSL/2 - [1] + [3])\}$. [c] See footnote *c* in Table 3. [d] Spectroscopic characteristics of transitions from the E_{2g} state.

and *C* terms. In addition, the transitions $G \longrightarrow E_1^{(-)}$ and $G \longrightarrow E_1^{(+)}$ have non-vanishing dipole strengths. They have positive *A* terms, dominated by the $\mu(n,N)$ contributions to their magnetic moments, and negative *C* terms. The *B* terms of the $E_1^{(-)}$ and $E_1^{(+)}$ states are due to their mutual magnetic mixing. The sign of the $E_1^{(-)}$ *B* term is equal to the sign of $2\mu(n,N) - \mu(n,N + 1)$, which is easily deduced as a function of *n* and *N* from the algebraic formulae given in the Appendix of ref. 8. The sign of the $E_1^{(+)}$ *B* term is the opposite.

4.5 4*N*-Electron [2*N* + 2]annulenes (*n* > 6)

In these anions (Table 10), the LO level is non-degenerate and the ε_{2N+1} configurations are absent. Three doubly degenerate excited states, $E_1^{(-)}$, E_{2N-1} and $E_1^{(+)}$ are obtained in addition to the ground state and the first excited state. The components of the E_{2N-1} state are Ψ_{-N+1}^{N} and Ψ_{N-1}^{-N}.

The $G \longrightarrow E_{2N-1}$ transition is allowed and shows the usual *A* and *C* terms. In addition, the transitions $G \longrightarrow E_1^{(-)}$ and $G \longrightarrow E_1^{(+)}$ have non-vanishing dipole strengths. They have negative *A* terms, dominated by the $\mu(n,N)$ contributions to their magnetic moments, and positive *C* terms. The *B* terms of the $G \longrightarrow E_1^{(-)}$ and $G \longrightarrow E_1^{(+)}$ transitions are due to the mutual magnetic mixing of their excited states. As $2\mu(n,N) - \mu(n,N - 1)$ is always negative, the *B* term for the lower state is always positive and that of the upper state is always negative. In the perfect alternant pairing approximation, the MCD spectra of a 4-electron [*n*]annulene polycation and a $(2n - 4)$-electron [*n*]annulene polyanion are mirror images of each other.[25]

4.6 4-Electron [6]annulene

Benzene dication (Table 11) differs from a general 4-electron [*n*]annulene in that the representations ε_{2N+1} (ε_3) and $\varepsilon_{-(2N+1)}$ (ε_{-3}) coincide to yield B in the C_6 symmetry group. The E_{2N+1} state splits into a lower $B^{(-)}$ and a higher $B^{(+)}$ state, as it does in other $4N$-electron $[4N + 2]$annulenes. The properties of the $E_1^{(-)}$ and $E_1^{(+)}$ states remain those of the general system, but the dipole strength and the *C* terms of the former E_{2N+1} state are split equally between the $B^{(-)}$ and $B^{(+)}$ states. Transitions $G \longrightarrow B^{(-)}$ and $G \longrightarrow B^{(+)}$ show nonvanishing B terms due to their mutual magnetic mixing, positive for $B^{(-)}$ and negative for $B^{(+)}$.

4.7 8-Electron [6]annulene

In benzene dianion (Table 12) the coalescence of the irreducible representations $\varepsilon_3 = \varepsilon_{2N-1}$ and $\varepsilon_{-3} = \varepsilon_{-(2N+1)}$ into B again leads to the splitting of the E_{2N-1} state present in the general $(2n - 4)$-electron [*n*]annulene. The dipole strength and the *C* terms are distributed equally to the resulting lower $B^{(-)}$ and upper $B^{(+)}$ states, which are the same as in general $4N$-electron $[4N - 2]$annulenes. Their mutual magnetic mixing produces a negative *B* term for the $B^{(-)}$ state and a positive one for $B^{(+)}$. The properties of the other states are as described for the general system. The MCD spectra of $C_6H_6^{2+}$ and $C_6H_6^{2-}$ are again paired in the perfect alternant pairing approximation.[25]

4.8 4*N*-Electron [4*N* + 1]annulenes (*n* > 6)

These antiaromatic monocations of odd-membered perimeters (Table 13) differ from general charged systems in that the representation $\varepsilon_{-(2N+1)}$ is the same as ε_{2N} in the C_{4N+1} symmetry group. The high-energy configuration Ψ_N^{-N-1} then interacts with the ground configuration Ψ_{-N}^{N}, as do the respective complex conjugates. The $E_{2N}^{(-)}$ ground state thus has an out-of-phase contribution from Ψ_{-N}^{N} (Ψ_N^{-N}) and Ψ_N^{-N-1} (Ψ_{-N}^{N+1}). The $E_1^{(-)}$, $E_1^{(+)}$ and E_{2N-1} states are not affected. The spectroscopic properties of the excited states change slightly.

The symmetry-allowed transitions are $G \longrightarrow E_{2N-1}$ and

Table 11 4-Electron [6]annulene dication [a,b]

State	Energy	D [d]	$\mathscr{M}$ [c,d]	B [d]	C [d]
E_{2g}	0	—	$2\mu(6,1)$	—	—
A_{1g}	[2]	0	0	0	0
$E_{1u}^{(+)}$	$c + [1]/\tan\beta - \Delta HSL/4 + [3]$	$2m^2(6,1)\cos^2\beta$	$-\mu(6,1)\cos 2\beta - \mu(6,2)\sin^2\beta$	$+\Delta^{-1}(E_{1u}^{(-)},E_{1u}^{(+)})[\mu(6,1) - (1/2)\mu(6,2)] \times \sin^2 2\beta m^2(6,1)$	$2\mu(6,1)\cos^2\beta m^2(6,1)$
$B_{1u}^{(-)}$	$c + [1] - [2] - [3] - \Delta HSL/4$	$m^2(6,3)$	0	$-\Delta^{-1}(B_{2u}^{(+)},B_{1u}^{(-)})[\mu(6,1) + \mu(6,2)] \times m^2(6,3)$	$-\mu(6,1)m^2(6,3)$
$E_{1u}^{(-)}$	$c - [1]\tan\beta - \Delta HSL/4 + [3]$	$2m^2(6,1)\sin^2\beta$	$\mu(6,1)\cos 2\beta - \mu(6,2)\cos^2\beta$	$-\Delta^{-1}(E_{1u}^{(-)},E_{1u}^{(+)})[\mu(6,1) - (1/2)\mu(6,2)] \times \sin^2 2\beta m^2(6,1)$	$2\mu(6,1)\sin^2\beta m^2(6,1)$
$B_{2u}^{(+)}$	$c + [1] + [2] + [3] - \Delta HSL/4$	$m^2(6,3)$	0	$\Delta^{-1}(B_{2u}^{(+)},B_{1u}^{(-)})[\mu(6,1) + \mu(6,2)] \times m^2(6,3)$	$-\mu(6,1)m^2(6,3)$

[a] See footnote *a* in Table 3. [b] $\beta = (1/2)\tan^{-1}\{2[1]/(\Delta HSL/2 + [1] - [3])\}$. [c] See footnote *c* in Table 3. [d] Spectroscopic characteristics of transitions from the E_{2g} state.

Table 12 8-Electron [6]annulene dianion [a,b]

State	Energy	D [d]	$\mathscr{M}$ [c,d]	B [d]	C [d]
E_{2g}	0	—	$2\mu(6,2)$	—	—
A_{1g}	[4]	0	0	0	0
$E_{1u}^{(-)}$	$c + [1](1 - \tan\beta) - \Delta HSL/4$	$2m^2(6,5)\cos^2\beta$	$\mu(6,2)\cos 2\beta + \mu(6,1)\sin^2\beta$	$-\Delta^{-1}(E_{1u}^{(+)},E_{1u}^{(-)})[\mu(6,2) - \mu(6,1)/2]\sin^2 2\beta m^2(6,5)$	$-2\mu(6,2)\cos^2\beta m^2(6,5)$
$B_{1u}^{(-)}$	$c + [1] - [3] - [4] + \Delta HSL/4$	$m^2(6,3)$	0	$-\Delta^{-1}(B_{2u}^{(+)},B_{1u}^{(-)})[\mu(6,2) + \mu(6,1)]m^2(6,3)$	$\mu(6,2)m^2(6,3)$
$E_{1u}^{(+)}$	$c + [1](1 + 1/\tan\beta) - \Delta HSL/4$	$2m^2(6,5)\sin^2\beta$	$-\mu(6,2)\cos 2\beta + \mu(6,1)\cos^2\beta$	$\Delta^{-1}(E_{1u}^{(+)},E_{1u}^{(-)})[\mu(6,2) - \mu(6,1)/2]\sin^2 2\beta m^2(6,5)$	$-2\mu(6,2)\sin^2\beta m^2(6,5)$
$B_{2u}^{(+)}$	$c + [1] + [3] + [4] + \Delta HSL/4$	$m^2(6,3)$	0	$-\Delta^{-1}(B_{2u}^{(+)},B_{1u}^{(-)})[\mu(6,2) + \mu(6,1)]m^2(6,3)$	$\mu(6,2)m^2(6,3)$

[a] See footnote *a* in Table 3. [b] See footnote *b* in Table 10. [c] See footnote *c* in Table 3. [d] Spectroscopic characteristics of transitions from the E_{2g} state.

Table 13 $4N$-Electron $[4N + 1]$annulene monocations ($N > 1$) [a,b]

State	Energy	D [d]	$\mathscr{M}$ [c,d]	B [d]	C [d]
$E_{2N}^{(-)}$	$\sqrt{2}[2N]\tan\alpha$	—	$(3\cos^2\alpha - 1)\mu - (1/2)(\mu_+ + \mu_-)\sin^2\alpha$	—	—
A	$[2N]$	0	0	0	0
$E_1^{(+)}$	$c - \Delta HSL/4 + [1]/\tan\beta + [2N + 1]$	0	$\mu_-/2 - \cos 2\beta(\mu_+/2 - \mu)$	0	0
E_{2N-1}	$c + \Delta HSL/4 + [1]$	$2m^2(n,2N - 1) \times \cos^2\alpha$	$-[\mu + (\mu_+ - \mu_-)/2]$	$\Delta^{-1}(E_{2N}^{(+)},E_{2N}^{(-)})\sin^2 2\alpha \times m^2(n,2N - 1)(1/2)[3\mu + (\mu_+ + \mu_-)/2]$	$[(3\cos^2\alpha - 1)\mu - (1/2) \times (\mu_+ + \mu_-)\sin^2\alpha] \times m^2(n,2N - 1)\cos^2\alpha$
$E_{2N}^{(+)}$	$-\sqrt{2}[2N]/\tan\alpha$	$2m^2(n,N + 1) \times \cos^2 2\alpha$	$-[(3\sin^2\alpha - 1)\mu - (1/2)(\mu_+ + \mu_-)\cos^2\alpha]$	0	$-[(3\cos^2\alpha - 1)\mu - (1/2) \times (\mu_+ + \mu_-)\sin^2\alpha]m^2(n,2N + 1)\cos^2 2\alpha$
$E_1^{(-)}$	$c - \Delta HSL/4 - [1]\tan\beta + [2N + 1]$	0	$\mu_-/2 + \cos 2\beta(\mu_+/2 - \mu)$	0	0

[a] See footnote *a* in Table 3. [b] $\alpha = (1/2)\tan^{-1}\{-2\sqrt{2}[2N]/(c - \Delta HSL/4 + [1])\}$; $\beta = (1/2)\tan^{-1}\{2[1]/(\Delta HSL/2 + [2N - 1] - [2N + 1])\}$. [c] See footnote *c* in Table 3. [d] Spectroscopic characteristics of transitions from the $E_{2N}^{(-)}$ state.

$G \longrightarrow E_{2N}^{(+)}$. Both have a positive A term. The former has a negative and the latter a positive C term. The former has a negative B term due to magnetic mixing of the two E_{2N} states, while the B term of the latter vanishes.

4.9 4*N*-Electron [4*N* − 1]annulenes (*n* > 6)

These antiaromatic monoanions of odd-membered perimeters (Table 14) differ from general charged systems in that $\varepsilon_{-(2N-1)}$ is the same representation as ε_{2N} in the C_{4N-1} symmetry group. The degenerate $E_{2N}^{(-)}$ ground state acquires an in-phase admixture of the high-energy Ψ_{-N+1}^{N}, Ψ_{N-1}^{-N} configurations. The excited states $E_1^{(-)}$, $E_1^{(+)}$ and E_{2N+1} are not affected.

The symmetry-allowed transitions are $G \longrightarrow E_{2N+1}$ and $G \longrightarrow E_{2N}^{(+)}$. The C term of the former is positive, that of the latter negative. The B term of the former, due to magnetic mixing of the E_{2N} states, is positive. The B term of the latter

Table 14 $4N$-Electron $[4N - 1]$annulene monoanions[a,b]

State	Energy	D[d]	$\mathcal{M}$[c,d]	B[d]	C[d]
$E_{2N}^{(-)}$	$-\sqrt{2}[2N]\tan\alpha$	—	$(3\cos^2\alpha - 1)\mu - (1/2) \times (\mu_+ - \mu_-)\sin^2\alpha$	—	—
A	$[2N]$	0	0	0	0
$E_1^{(-)}$	$c - \Delta HSL/4 - [1]\tan\beta + [2N + 1]$	0	$\mu_-/2 - \cos 2\beta(\mu - \mu_+/2)$	0	0
E_{2N+1}	$c - \Delta HSL/4 + [1]$	$2m^2(n,2N + 1) \times \cos^2\alpha$	$\mu + (1/2)(\mu_+ + \mu_-)$	$-\Delta^{-1}(E_{2N}^{(+)},E_{2N}^{(-)})(1/2) \times \sin^2 2\alpha\, m^2(n,2N + 1) \times [3\mu + (\mu_+ - \mu_-)/2] \times [(\mu_+ - \mu_-)\sin^2\alpha]$	$-[(3\cos^2\alpha - 1)\mu - (1/2)(\mu_+ - \mu_-)\sin^2\alpha] m^2(n,2N + 1) \times \cos^2\alpha$
$E_{2N}^{(+)}$	$\sqrt{2}[2N]/\tan\alpha$	$2m^2(n,2N - 1) \times \cos^2 2\alpha$	$(3\sin^2\alpha - 1)\mu - (1/2) \times (\mu_+ - \mu_-)\cos^2\alpha$	0	$[(3\cos^2\alpha - 1)\mu - (1/2)(\mu_+ - \mu_-) \times \sin^2\alpha]m^2(n,2N - 1) \times \cos^2 2\alpha$
$E_1^{(+)}$	$c - \Delta HSL/4 + [2N + 1] + [1]/\tan\beta$	0	$\mu_-/2 + \cos 2\beta(\mu - \mu_+/2)$	0	0

[a] See footnote *a* in Table 3. [b] $\alpha = (1/2)\tan^{-1}\{2\sqrt{2}[2N]/(c + \Delta HSL/4 + [1])\}$; $\beta = (1/2)\tan^{-1}\{2[1]/(\Delta HSL/2 + [2N - 1] - [2N + 1])\}$. [c] See footnote *c* in Table 3. [d] Spectroscopic characteristics of transitions from the $E_{2N}^{(-)}$ state.

Table 15 $2N$-Electron $[2N + 1]$annulene anions $(N > 2)$[a,b]

State	Energy	D[d]	$\mathcal{M}$[c,d]	B[d]	C[d]
$E_1^{(-)}$	$-\sqrt{2}[1]\tan\alpha$	—	$(2\mu\cos 2\alpha + \sin^2\alpha)[\mu + \mu(n,N - 1)]$	—	—
A	$[2N]$	D_A[e]	0	B_A[f]	$-(1/2)\mu(1 + \cos^2\alpha) \times D_A$[e]
E_{2N-1}	$E(\mathrm{SO}) - E(\mathrm{HO}) + [1]$	D_E[g]	$-[\mu + \mu(n,N - 1)]$	B_E[h]	$(1/2)\mu(1 + \cos^2\alpha) \times D_E$[g]
$E_1^{(+)}$	$\sqrt{2}[1]/\tan\alpha$	0	$(2\mu\cos 2\alpha - \cos^2\alpha)[\mu + \mu(n,N - 1)]$	0	0

[a] See footnote *a* in Table 3. [b] $\alpha = (1/2)\tan^{-1}(2\sqrt{2}[1]/\{E(\mathrm{SO}) - E(\mathrm{HO}) + [2N - 1]\})$. [c] See footnote *c* in Table 3. [d] Spectroscopic characteristics of transitions from the $E_1^{(-)}$ state. [e] $D_A = [\cos\alpha\ \sqrt{2}\, m(n,2N + 1) - \sin\alpha\ \ m(n,2N - 1)]^2$. [f] $B_A = \Delta^{-1}(E_1^{(+)},E_1^{(-)})[-3\mu + \mu(n,N - 1)](1/2)\sin 2\alpha \times \{\sin 2\alpha[m^2(n,2N + 1) - (1/2)m^2(n,2N - 1)] + \cos 2\alpha\ \ \sqrt{2}m(n,2N + 1) \times m(n,2N - 1)\}$. [g] $D_E = [\cos\alpha\ \ \sqrt{2}m(n,2N - 1) - \sin\alpha\, m(n,2N + 1)]^2$. [h] $B_E = -\Delta^{-1}(E_1^{(+)},E_1^{(-)})[-3\mu + \mu(n,N - 1)](1/2)\sin 2\alpha \times \{\sin 2\alpha[m^2(n,2N - 1) - (1/2)m^2(n,2N + 1)] + \cos 2\alpha\ \sqrt{2}m(n,2N + 1) \times m(n,2N - 1)\}$.

Table 16 4-Electron [3]annulene monoanion[a,b]

State	Energy	D[d]	$\mathcal{M}$[c,d]	B[d]	C[d]
$E_1^{(-)}$	$-\sqrt{2}[1]\tan\alpha$	—	$\mu(1 - 3\cos^2\alpha)$	—	—
A	[2]	$[\sqrt{2}\cos\alpha\, m(3,3) - \sin\alpha\, m(3,1)]^2$	0	B_A[e]	C_A[f]
$E_1^{(+)}$	$\sqrt{2}[1]/\tan\alpha$	$[\sqrt{2}\cos\alpha\, m(3,1) - (1/2)\sin 2\alpha \times m(3,3)]^2$	$-\mu(1 - 3\sin^2\alpha)$	B_E[g]	C_E[h]

[a] See footnote *a* in Table 3. [b] $\alpha = (1/2)\tan^{-1}(2\sqrt{2}[1]/\{E(\mathrm{SO}) - E(\mathrm{HO}) + [1]\})$. [c] See footnote *c* in Table 3. [d] Spectroscopic characteristics of transitions from the $E_1^{(-)}$ state. [e] $B_A = -\Delta^{-1}(E_1^{(+)},E_1^{(-)})(3/2)\mu\sin 2\alpha \times \{\sin 2\alpha[m^2(3,3) - (1/2)m^2(3,1)] + \cos 2\alpha\ \ \sqrt{2}m(3,3)m(3,1)\}$. [f] $C_A = (1/2)\mu(1 - 3\cos^2\alpha)[\sqrt{2}\cos\alpha\ \ m(3,3) - \sin\alpha\ \ m(3,1)]^2$. [g] $B_E = -\Delta^{-1}(E_1^{(+)},E_1^{(-)}) \times (3/2)\mu\sin 2\alpha[-\sqrt{2}m(3,1)\cos 2\alpha + (1/2)\sin 2\alpha \times m(3,3)]m(3,3)$. [h] $C_E = -(1/2) \times \mu(1 - 3\cos^2\alpha)[(1/2)\sin 2\alpha\, m(3,3) - \sqrt{2}\cos 2\alpha\, m(3,1)]^2$.

vanishes. The signs of the B and C terms are just the opposite of those obtained for the $4N$-electron $[4N + 1]$annulenes. The sign of the A term of the $G \longrightarrow E_{2N+1}$ transition is negative for small n and positive for large n, and the A term of the $G \longrightarrow E_{2N}^{(+)}$ transition is positive.

4.10 $4N$-Electron $[2N + 1]$annulenes ($n > 6$)

In these systems (Table 15) the SO level corresponds to the highest energy pair of orbitals and no LO level is present, leaving only the HO $\longrightarrow$ SO excitations. The irreducible representations ε_{2N} and ε_{-2N} are equal to ε_{-1} and ε_1, respectively, and the low-energy configuration Ψ_{-N}^{N} interacts with the high-energy configuration Ψ_{-N+1}^{-N}, as do their complex conjugates. The high-energy configurations mix in-phase into the $E_1^{(-)}$ ground state, while the low-energy configurations mix out-of-phase into the $E_1^{(+)}$ excited state.

This configuration mixing introduces a highly unusual non-vanishing dipole strength and a positive C and negative A term for the transition $G \longrightarrow A$. The $G \longrightarrow E_{2N-1}$ transition is electric dipole allowed, with negative A and C terms.

4.11 4-Electron [3]annulene

The cyclopropenide anion (Table 16) represents a special case of $4N$-electron $[2N + 1]$annulene because the LO level is missing and the HO level is non-degenerate. Only five configurations are left. The wavefunctions and spectroscopic properties are those of a general $4N$-electron $[2N + 1]$annulenes, except that the E_{2N-1} state is absent.

4.12 4-Electron [5]annulene

The cyclopentadienyl cation (Table 17) differs from the general 4-electron [*n*]annulene only in the fact that E_{2N} and E_{-2N+1} coincide in the C_5 symmetry group, causing Ψ_{-N}^{N} and Ψ_{N}^{-N-1}, and their complex conjugates, to interact. The interaction yields a $E_2^{(-)}$ ground state and an excited $E_2^{(+)}$ state. The other states are not affected.

Table 17 4-Electron [5]annulene[a,b]

State	Energy	D^d	$\mathcal{M}^{c,d}$	B^d	C^d
$E_2^{(+)}$	$\sqrt{2}[2]\tan\alpha$	—	$\mu(5,1)(3\cos^2\alpha - 1) - \mu(5,2)\sin^2\alpha$	—	—
A	[2]	0	0	0	0
$E_1^{(+)}$	$c - \Delta HSL/4 + [1]/\tan\beta + [2]$	$[\cos\alpha\cos\beta\sqrt{2}m(5,1) - \sin\alpha\sin\beta\, m(5,5)]^2$	$-\mu(5,1)\cos 2\beta - \mu(5,2)\sin^2\beta$	$B_{1+}{}^e$	$C_{1+}{}^e$
$E_2^{(-)}$	$-\sqrt{2}[2]/\tan\alpha$	$2\cos^2 2\alpha\, m^2(5,3)$	$-\mu(5,1)(3\sin^2\alpha - 1) + \mu(5,2)\cos^2\alpha$	0	$C_{2-}{}^e$
$E_1^{(-)}$	$c - \Delta HSL/4 - [1]\tan\beta + [2]$	$[\cos\alpha\sin\beta\sqrt{2}m(5,1) + \sin\alpha\cos\beta\, m(5,5)]^2$	$\mu(5,1)\cos 2\beta - \mu(5,2)\cos^2\beta$	$B_{1-}{}^e$	$C_{1-}{}^e$

[a] See footnote *a* in Table 3. [b] $\beta = (1/2)\tan^{-1}\{2[1]/(\Delta HSL/2 + [1] - [2])\}$; $\alpha = (1/2)\tan^{-1}\{-2\sqrt{2}[2]/(c - \Delta HSL/4 + [1])\}$. [c] See footnote *c* in Table 3. [d] Spectroscopic characteristics of transitions from the $E_2^{(+)}$ state. [e] The following abbreviations are used: $B_{1-} = \Delta^{-1}(E_2^{(-)},E_2^{(+)})(1/2) \times \sin 2\alpha[3\mu(5,1) + \mu(5,2)][\cos\alpha\sin\beta\sqrt{2}m(5,1) + \sin\alpha\cos\beta m(5,5)][-\cos\beta\cos\alpha m(5,5) + \sin\beta\sin\alpha\sqrt{2}m(5,1)] - \Delta^{-1}(E_1^{(+)},E_1^{(-)})(1/2)\sin 2\beta[2\mu(5,1) - \mu(5,2)](\cos\alpha\sin\beta\sqrt{2}m(5,1) + \sin\alpha\cos\beta m(5,5)][-\cos\alpha\cos\beta\sqrt{2}m(5,1) + \sin\alpha\sin\beta m(5,5)]$; $B_{1+} = \Delta^{-1}(E_1^{(+)},E_1^{(-)})(1/2)\sin 2\beta[2\mu(5,1) - \mu(5,2)] \times [\cos\alpha\sin\beta\sqrt{2}m(5,1) + \sin\alpha\cos\beta m(5,5)][-\cos\alpha\cos\beta\sqrt{2}m(5,1) + \sin\alpha\sin\beta m(5,5)] - \Delta^{-1}(E_2^{(-)},E_2^{(+)})(1/2)\sin 2\alpha[3\mu(5,1) + \mu(5,2)][-\cos\alpha\cos\beta \times \sqrt{2}m(5,1) + \sin\alpha\sin\beta m(5,5)][\sin\alpha\cos\beta\sqrt{2}m(5,1) + \cos\alpha\sin\beta m(5,5)]$; $C_{1-} = (1/2)[\mu(5,1)(3\cos^2\alpha - 1) - \sin^2\alpha\mu(5,2)][\cos\alpha\sin\beta\sqrt{2}m(5,1) + \sin\alpha\cos\beta m(5,5)]$; $C_{2-} = -[\mu(5,1)(3\cos^2\alpha - 1) - \sin^2\alpha\mu(5,2)]\cos^2 2\alpha m^2(5,3)$; $C_{1+} = (1/2)[\mu(5,1)(3\cos^2\alpha - 1) - \sin^2\alpha\mu(5,2)][-\cos\alpha\cos\beta\sqrt{2}m(5,1) + \sin\alpha\sin\beta m(5,5)]^2$.

The modified ground state still has a vanishing transition moment for G ⟶ A. All other transitions are allowed and show positive *A* terms for the $E_1^{(-)}$ and $E_1^{(+)}$ states and a negative *A* term for the $E_2^{(-)}$ state. The signs of the *C* terms are the opposite of those of the *A* terms. The *B* terms of the transitions to the lower $E_1^{(+)}$ and upper $E_1^{(-)}$ states are due to their mutual magnetic mixing. The former is negative and the latter positive.

5. Magnetic circular dichroism of antiaromatic perturbed 4*N*-electron [*n*]annulenes

The procedure that shall be used to describe the structural factors which distinguish the π system of an actual molecule from that of the idealized perimeter has already proven its value in the case of aromatic π systems.[8–11] Its most important simplifying features are that only the one-electron part of the perturbation and only the mixing between degenerate orbitals are considered.

Those perturbations of a 4*N*-electron [*n*]annulene perimeter which preserve its biradicaloid and antiaromatic nature are considered next, while those stronger perturbations which convert it into ordinary (unaromatic) molecules are considered in Parts 2 and 3. Examples of perturbations considered now are geometrical distortions, attachment of weakly perturbing substituents, and other minor modifications that split the degeneracy of the SO level only very weakly or not at all, and also those strong perturbations, such as cross-links, whose symmetry is such that the degeneracy of the SO level is preserved.

The Hamiltonian matrix of a perturbed system differs in several respects from that of the parent antiaromatic annulene given in expression (9). Considering only the one-electron part of the perturbation and representing it by the operator $\hat{A} = \Sigma_i \hat{a}_i$, these are: (i) changes in the energy zero and in *c*, of little interest presently, (ii) a change in Δ*HSL*, (iii) appearance of non-zero values for the perturbation parameters *h*, *s* and *l*.

The change in Δ*HSL* is given by the diagonal elements of $\hat{a}$, eqn. (20).

$$2\langle\psi_N|\hat{a}|\psi_N\rangle - \langle\psi_{N-1}|\hat{a}|\psi_{N-1}\rangle - \langle\psi_{N+1}|\hat{a}|\psi_{N+1}\rangle = 2s_D - h_D - l_D \quad (20)$$

The perturbation parameters *h*, *s* and *l* are given by the off-diagonal elements of $\hat{a}$, eqn. (21).

$$h = \langle\psi_{N-1}|\hat{a}|\psi_{-N+1}\rangle = \Delta H e^{i\eta}/2$$
$$s = \langle\psi_N|\hat{a}|\psi_{-N}\rangle = \Delta S e^{i\sigma}/2$$
$$l = \langle\psi_{N+1}|\hat{a}|\psi_{-N-1}\rangle = \Delta L e^{i\lambda}/2 \quad (21)$$

The real and positive quantities Δ*H*, Δ*S* and Δ*L* are given by the splitting of the HO, SO and LO orbital pairs, respectively, under the effect of the perturbation, while the phase angles η, σ and λ specify its symmetry properties. A detailed discussion of these quantities will be postponed until Parts 2 and 3.

It is useful to consider separately the effects of high-symmetry perturbations which preserve a symmetry axis of order three or higher, and of low-symmetry perturbations, which do not. High-symmetry perturbations can be classified further according to their effect on Δ*H*, Δ*S* and Δ*L*, *i.e.* their effect on the degeneracy of the HO, SO and LO levels. Table 18 shows the effect of reducing the order of the symmetry axis from *n* to *n*/*m*.

5.1 High-symmetry antiaromatic biradicals

Reduction of symmetry from C_n to $C_{n/m}$ which keeps SO degenerate ($\Delta S = 0$) converts a 4*N*-electron [*n*]annulene perimeter into another antiaromatic perfect biradical. Within the present model, a perturbation of this symmetry, for which $\Delta S = 0$, cannot change the nature of the lowest three singlets regardless of its strength, since the 3 × 3 matrix block remains independent of the perturbation and is not coupled to the remaining 8 × 8 block of the matrix except in the case of singly charged perimeters, and even there the coupling is nearly negligible.

For certain limiting cases, an explicit solution for wave functions and spectroscopic observables, including MCD, is easy. This happens when, in addition to $\Delta S = 0$, either $\Delta L = 0$ or $\Delta H = 0$ or $\Delta L = \Delta H$ holds, with either $\eta = \lambda$ or $\eta = \lambda + \pi$. The vanishing of Δ*L* or Δ*H* may be imposed by geometrical symmetry (Table 18). The condition $\Delta L = \Delta H$ may be imposed to a good approximation in systems which are alternant, or to first order in perturbation theory in systems derived by a purely even or purely odd perturbation[5] of an uncharged antiaromatic perimeter. We shall not present the detailed solutions here.

In the general case, however, the solutions cannot be written down explicitly and the matrix must be diagonalized numerically. It may still be possible to understand trends in the results by comparison with related simply soluble limiting cases.

Biradicals of this type are still subject to a Jahn–Teller distortion if their singlet ground state is degenerate and to a pseudo-Jahn–Teller distortion if it is not.

5.2 High-symmetry antiaromatic biradicaloids

Reduction of symmetry from C_n to $C_{n/m}$ ($n/m \geqslant 3$) which splits the degeneracy of SO ($\Delta S \neq 0$, $\Delta H = \Delta L = 0$, Table 18)

Table 18 Lifting of orbital degeneracy in [*n*]annulenes upon symmetry reduction $C_n \longrightarrow C_{n/m}$ ($n/m \geqslant 3$)

			Charge required[a]		
$(CH)_n$	n/m	k[b]	$\Delta H \neq 0$	$\Delta S \neq 0$	$\Delta L \neq 0$
C_8H_8	4	2	4−	0	4+
C_9H_9	3	3	7−	3−	1+
$C_{12}H_{12}$	3, 6	3	4−	0	4+
$C_{12}H_{12}$	4	2, 4	0, 8−	4+, 4−	8+, 0
$C_{15}H_{15}$	3	3, 6	1−, 13−	3+, 9−	7+, 5−
$C_{15}H_{15}$	5	5	9−	5−	1−
$C_{16}H_{16}$	4	2, 4, 6	4+, 4−, 12−	8+, 0, 8−	12+, 4+, 4−
$C_{16}H_{16}$	8	4	4−	0	4+
$C_{18}H_{18}$	3, 6	3, 6	2+, 10−	6+, 6−	10+, 2−
$C_{20}H_{20}$	4	2, 4, 6, 8	8+, 0, 8−, 16−	12+, 4+, 4−, 12−	16+, 8+, 0, 8−
$C_{20}H_{20}$	5, 10	5	4−	0	4+
$C_{21}H_{21}$	3	3, 6, 9	5+, 7−, 19−	9+, 3−, 15−	13+, 1+, 11−
$C_{21}H_{21}$	7	7	11−	7−	3−

[a] The charge on the annulene required to achieve $\Delta H \neq 0$, $\Delta S \neq 0$ or $\Delta L \neq 0$. [b] Subscript of the orbital pairs ψ_k, ψ_{-k} that split.

Table 19 Antiaromatic high-symmetry perturbed 4*N*-electron [4*N*]annulenes with $\sigma = 0$ (weakly heterosymmetric biradicaloids, $\Delta H = \Delta L = \Delta HSL = 0$, $0 < \Delta S < 2[2N]$)[a,b]

State	Energy and symmetry at $\Delta S = 0$		Energy	D[d]	$\mathscr{M}$[c]	B[d]
G	$-[2N]\ B_{1g}^{(-)}$		$-[2N]$	—	0	—
S	$+[2N]\ B_{2g}^{(+)}$		$[2N] - \Delta S$	0	0	0
D	$+[2N]\ A_{1g}^{(-)}$		$[2N] + \Delta S$	0	0	0
N	$c + [2N - 1] - [1]$	$E_{1u}^{(-)}$	$c + [2N - 1] - [1] - (\Delta S/2)\tan\beta$	$m_+^2 \sin^2\beta$	$\mu_-/2$	$B_{DG}^{N} + B_{SG}^{N} + B_{PN}^{N} + B_{P'N}^{N}$[e]
P	$c - [2N - 1] + [1]$	$E_{2N+1,u}^{(-)}$	$c - [2N - 1] + [1] - (\Delta S/2)\tan\gamma$	$m_-^2 \cos^2\gamma$	$\mu_-/2$	$B_{DG}^{P} + B_{SG}^{P} + B_{NP}^{P} + B_{N'P}^{P}$[f]
N′	$c + [2N - 1] + [1]$	$E_{2N+1,u}^{(+)}$	$c + [2N - 1] + [1] + (\Delta S/2)\tan\beta$	$m_+^2 \cos^2\beta$	$\mu_-/2$	$B_{DG}^{N'} + B_{SG}^{N'} + B_{PN'}^{N'} + B_{P'N'}^{N'}$[g]
P′	$c + [2N-1] + [1]$	$E_{1u}^{(+)}$	$c + [2N - 1] + [1] + (\Delta S/2)\tan\gamma$	$m_-^2 \sin^2\gamma$	$\mu_-/2$	$B_{DG}^{P'} + B_{SG}^{P'} + B_{NP'}^{P'} + B_{N'P'}^{P'}$[h]

[a] See footnote *a* in Table 3. [b] $\beta = (1/2)\tan^{-1}(\Delta S/2[1])$; $\gamma = (1/2)\tan^{-1}(\Delta S/2[2N - 1])$; $\beta' = \beta + \pi/4$; $\gamma' = \gamma + \pi/4$. [c] See footnote *c* in Table 3. [d] Spectroscopic characteristics of transitions from the G state. [e] $B_{DG}^{N} = \sqrt{2}\Delta^{-1}(D,G)\mu m_+m_-\cos\beta'\sin\beta$; $B_{SG}^{N} = -\sqrt{2}\Delta^{-1}(S,G)\mu m_+m_-\sin\beta'\sin\beta$; $B_{PN}^{N} = -\Delta^{-1}(P,N) \times [(\mu_+/2)\sin(\beta + \gamma) + \mu\sin(\beta - \gamma)]m_+m_-\sin\beta\cos\gamma$; $B_{P'N}^{N} = -\Delta^{-1}(P',N)[-(\mu_+/2)\cos(\beta + \gamma) + \mu\cos(\beta - \gamma)]m_+m_-\sin\beta\sin\gamma$. [f] $B_{DG}^{P} = -\sqrt{2}\Delta^{-1}(D,G) \times \mu m_+m_-\cos\gamma\cos\gamma'$; $B_{SG}^{P} = -\sqrt{2}\Delta^{-1}(S,G)\mu m_+m_-\cos\gamma\sin\gamma'$; $B_{NP}^{P} = \Delta^{-1}(P,N)[(\mu_+/2)\sin(\beta + \gamma) + \mu\sin(\beta - \gamma)]m_+m_-\sin\beta\cos\gamma = -B_{PN}^{N}$; $B_{N'P}^{P} = -\Delta^{-1}(N',P)[(\mu_+/2)\cos(\beta + \gamma) + \mu\cos(\beta - \gamma)]m_+m_-\cos\beta\cos\gamma$. [g] $B_{DG}^{N'} = -\sqrt{2}\Delta^{-1}(D,G)\mu m_+m_-\sin\beta'\cos\beta$; $B_{SG}^{N'} = -\sqrt{2}\Delta^{-1}(S,G)\mu m_+m_-\cos\beta'\cos\beta$; $B_{PN'}^{N'} = \Delta^{-1}(N',P)[(\mu_+/2)\cos(\beta + \gamma) + \mu\cos(\beta - \gamma)]m_+m_-\cos\beta\cos\gamma = -B_{N'P}^{P}$; $B_{P'N'}^{N'} = -\Delta^{-1}(P',N')[(\mu_+/2)\sin(\beta + \gamma) - \mu\sin(\beta - \gamma)]m_+m_-\cos\beta\sin\gamma$. [h] $B_{DG}^{P'} = -\sqrt{2}\Delta^{-1}(D,G)\mu m_+m_-\sin\gamma'\sin\gamma$; $B_{SG}^{P'} = \sqrt{2}\Delta^{-1}(S,G)\mu m_+m_-\cos\gamma'\sin\gamma$; $B_{NP'}^{P'} = \Delta^{-1}(P',N)[-(\mu_+/2)\cos(\beta + \gamma) + \mu\cos(\beta - \gamma)] \times m_+m_-\sin\beta\sin\gamma = -B_{P'N}^{N}$; $B_{N'P'}^{P'} = \Delta^{-1}(P',N')[(\mu_+/2)\sin(\beta + \gamma) - \mu\sin(\beta - \gamma)]m_+m_-\cos\beta\sin\gamma = -B_{P'N'}^{N'}$.

converts the antiaromatic perimeter from a perfect biradical to a biradicaloid. As long as ΔS is relatively small, $\Delta S < 2[2N]$, the molecule remains antiaromatic and all eleven configurations considered presently need to be kept. By a suitable choice of an atom numbering system, it is possible to force σ to become equal to an integral multiple of $\pi/2$ as long as at least one symmetry plane perpendicular to the annulene ring is present (see Parts 2 and 3 for more detail).

For an uncharged perimeter, it is then possible to find explicit solutions for the ground and excited state wavefunctions and spectroscopic properties, and the latter are given in Tables 19–21. Note that the spectroscopic properties of a heterosymmetric[12] biradicaloid ($\sigma = 0$) change discontinuously at $\Delta S = 2[2N]$ since the nature of the ground state changes abruptly (Table 19, $0 < \Delta S < 2[2N]$; Table 20, $\Delta S > 2[2N]$). Systems of this kind will be prone to a pseudo-Jahn–Teller distortion.

We have not found a simple closed-form solution for the case of a charged perimeter and a numerical diagonalization is necessary.

In more strongly perturbed high-symmetry systems ($\Delta S > 2[2N]$) only seven of the eleven configurations need to be kept. These molecules are called unaromatic [or ambiaromatic, if they can equally well be derived from a $(4N + 2)$-electron perimeter]. Explicit solutions for uncharged as well as charged perimeters are given in Parts 2 and 3.

5.3 Low-symmetry antiaromatic biradicals and biradicaloids

More general weak perturbations ($\Delta S < 2[2N]$; ΔL or $\Delta H \neq 0$) lead to Hamiltonian matrices which can only be diagonalized numerically. By introducing the perturbation gradually it may be possible to relate the results to one of the algebraically soluble cases listed above. This will provide insight into trends in the results as well as a correlation to the states of the parent perimeter, thus providing labels and nomenclature.

As soon as the perturbation is strong ($\Delta S > 2[2N]$), the molecule is unaromatic (or ambiaromatic). Then, it is possible to discard four of the eleven configurations and solve explicitly for many cases of interest (Parts 2 and 3).

6. Comparison with numerical calculations and summary

Results of PPP calculations of state energies and symmetries for a series of fourteen molecules selected for testing and illustration, performed using standard parameters[29] and the same eleven configurations, are shown in Fig. 3. The calculated dipole strengths and MCD *A*, *B* and *C* terms, which are not shown, support fully the results obtained from the perimeter model. Since the PPP model[30] is well known to give excellent results for $\pi\pi^*$ states of cyclic π-electron systems, this lends additional support to the perimeter model analysis. For several of the smallest antiaromatic perimeters good quality *ab initio*

Table 20 Unaromatic high-symmetry perturbed 4*N*-electron [4*N*]annulenes with $\sigma = 0$ (strongly heterosymmetric biradicaloids, $\Delta H = \Delta L = \Delta HSL = 0$, $\Delta S > 2[2N]$)[a,b]

State	Energy and symmetry at $\Delta S = 0$		Energy	D[c]	$\mathcal{M}$[d]	B[c]
G	$[2N]\ B_{2g}^{(+)}$		$[2N] - S$	—	0	—
S	$-[2N]\ B_{1g}^{(-)}$		$-[2N]$	0	0	0
D	$[2N]\ A_{1g}^{(-)}$		$[2N] + \Delta S$	0	0	0
N	$c + [2N-1] - [1]$	$E_{1u}^{(-)}$	$c + [2N-1] - [1] - (\Delta S/2)\tan\beta$	$m_-^2 \sin^2\beta'$	$\mu_-/2$	$B_{SG}^{N} + B_{PN}^{N} + B_{P'N}^{N}$[e]
P	$c - [2N-1] + [1]$	$E_{2N+1,u}^{(-)}$	$c - [2N-1] + [1] - (\Delta S/2)\tan\gamma$	$m_+^2 \sin\gamma'$	$\mu_-/2$	$B_{SG}^{P} + B_{NP}^{P} + B_{N'P}^{P}$[f]
N′	$c + [2N-1] + [1]$	$E_{2N+1,u}^{(+)}$	$c + [2N-1] + [1] + (\Delta S/2)\tan\beta$	$m_-^2 \cos^2\beta'$	$\mu_-/2$	$B_{SG}^{N'} + B_{PN'}^{N'} + B_{P'N'}^{P'}$[g]
P′	$c + [2N-1] + [1]$	$E_{1u}^{(+)}$	$c + [2N-1] + [1] + (\Delta S/2)\tan\gamma$	$m_+^2 \cos^2\gamma'$	$\mu_-/2$	$B_{SG}^{P'} + B_{N'P'}^{P'} + B_{NP'}^{P'}$[h]

[a] See footnote *a* in Table 3. [b] $\beta = (1/2)\tan^{-1}(\Delta S/2[1])$; $\gamma = (1/2)\tan^{-1}(\Delta S/2[2N-1])$; $\beta' = \beta + \pi/4$; $\gamma' = \gamma + \pi/4$. [c] Spectroscopic characteristics of transitions from the G state. [d] See footnote *c* in Table 3. [e] $B_{SG}^{N} = -\Delta^{-1}(S,G)(\sqrt{2})\mu m_+ m_- \sin\beta' \sin\beta$; $B_{PN}^{N} = -\Delta^{-1}(P,N)[(\mu_+/2)\ \sin(\beta+\gamma) + \mu \sin(\beta-\gamma)]m_+ m_- \sin\beta' \sin\gamma'$; $B_{P'N}^{N} = -\Delta^{-1}(P',N)[(\mu_+/2)\cos(\beta+\gamma) - \mu\cos(\beta-\gamma)]m_+ m_- \sin\beta' \cos\gamma'$. [f] $B_{SG}^{P} = -\Delta^{-1}(S,G)(\sqrt{2})\mu m_+ m_- \sin\gamma' \cos\gamma$; $B_{NP}^{P} = -B_{PN}^{N} = \Delta^{-1}(P,N)[(\mu_+/2)\sin(\beta+\gamma) + \mu\sin(\beta-\gamma)]m_+ m_- \sin\beta' \sin\gamma'$; $B_{N'P}^{P} = -\Delta^{-1}(N',P)[(\mu_+/2)\cos(\beta+\gamma) + \mu\cos(\beta-\gamma)]m_+ m_- \cos\beta' \sin\gamma'$. [g] $B_{SG}^{N'} = -\Delta^{-1}(S,G)(\sqrt{2})\mu m_+ m_- \cos\beta' \cos\beta$; $B_{PN'}^{N'} = -B_{N'P}^{P} = \Delta^{-1}(N',P)[(\mu_+/2)\cos(\beta+\gamma) + \mu\cos(\beta-\gamma)]m_+ m_- \cos\beta' \sin\gamma'$; $B_{P'N'}^{N'} = \Delta^{-1}(P',N')[(\mu_+/2)\sin(\beta+\gamma) - \mu\sin(\beta-\gamma)]m_+ m_- \cos\beta' \cos\gamma'$. [h] $B_{SG}^{P'} = \Delta^{-1}(S,G)\ (\sqrt{2})\mu m_+ m_- \cos\gamma' \sin\gamma$; $B_{N'P'}^{P'} = -B_{P'N'}^{N'} = -\Delta^{-1}(P',N')[(\mu_+/2)\sin(\beta+\gamma) - \mu\sin(\beta-\gamma)]m_+ m_- \cos\beta' \cos\gamma'$; $B_{NP'}^{P'} = -B_{P'N}^{N} = \Delta^{-1}(P',N)[(\mu_+/2)\cos(\beta+\gamma) - \mu\cos(\beta-\gamma)]m_+ m_- \sin\beta' \cos\gamma'$.

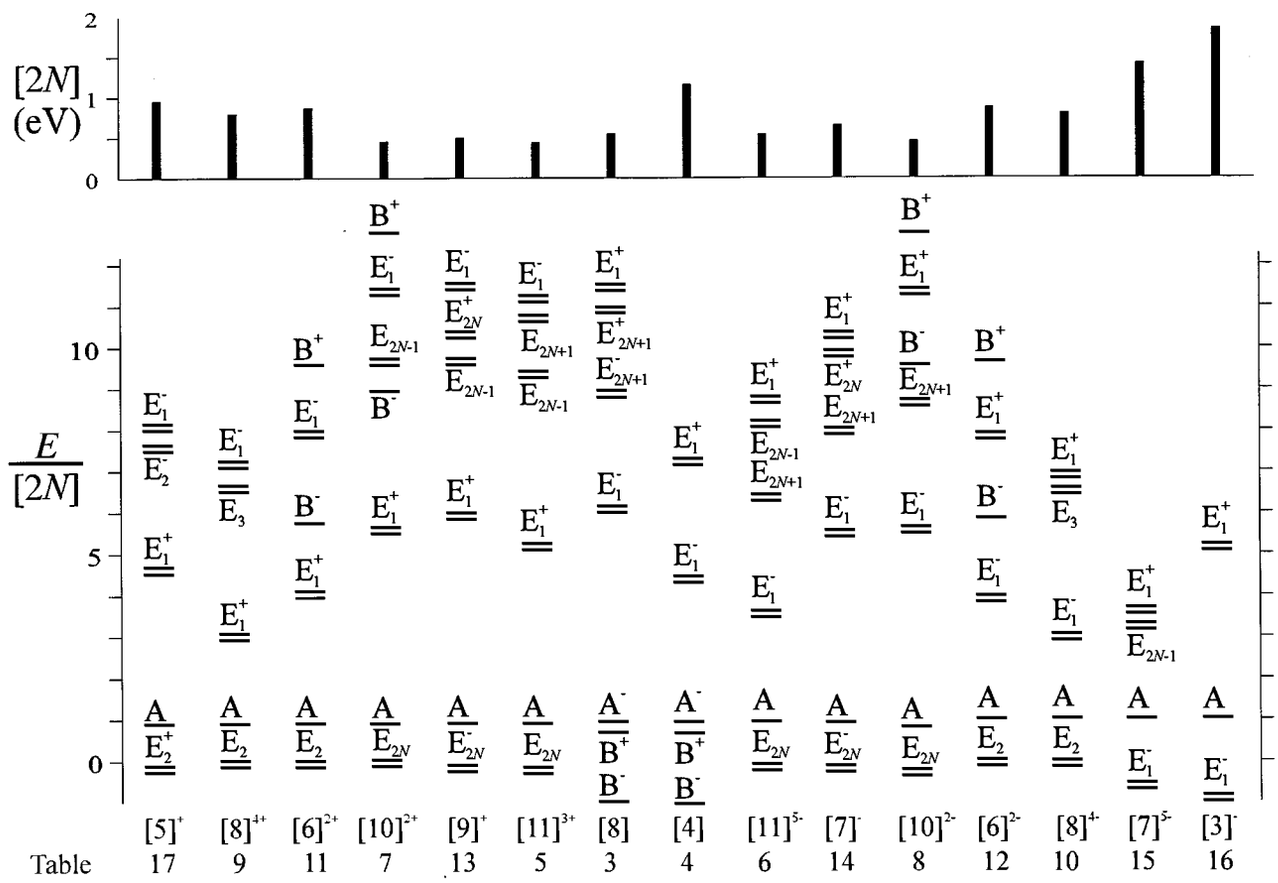

Fig. 3 Energies of the electronic states of 4*N*-electron [*n*]annulenes of D_{nh} symmetry in the PPP approximation, in units of [2*N*]. At the bottom, *n* and the charge are indicated. On top, the magnitude of [2*N*] in eV is shown for each case.

calculations of state energies and symmetries have been published.[18] Once again, these agree with the results of the perimeter model.

Although measurements on D_{nh} geometry systems will be complicated in practice by Jahn–Teller and pseudo-Jahn–Teller effects, the results for this idealized geometry will serve as a starting point for the treatment of the spectra of real molecular systems. In some cases it appears that the A singlet is the true experimental ground state.[28] Then, the present results should be applicable directly.

In addition to working out the spectroscopic properties, and in particular the MCD spectra to be expected for the parent antiaromatic annulenes, we have also considered those perturbations which preserve their antiaromatic biradical or biradicaloid nature. Very few antiaromatic biradicals and biradicaloids have been adequately characterized experimentally so far, and virtually no MCD spectra have been reported. The present results should be helpful in the detection of such molecules and in the determination of the nature of their ground electronic state.

The extension of the present results for idealized perimeters to more strongly perturbed 4*N*-electron perimeters, *i.e.* to unaromatic (or ambiaromatic) molecules, is presented in Parts 2 and 3. It is of greater practical importance than the present

Table 21 High-symmetry $4N$-electron [$4N$]annulene, biradicaloids with $\sigma = \pi/2$ ($\Delta H = \Delta L = \Delta HSL = 0$, $\Delta S \neq 0$) [a,b]

State	Energy and symmetry at $\Delta S = 0$		Energy	D [c]	$\mathcal{M}$ [d]	B [c]
G	$-[2N]\ B_{1g}^{(-)}$		$-[2N] - \Delta S \tan\alpha$	—	0	—
S	$+[2N]\ B_{2g}^{(+)}$		$[2N]$	0	0	0
D	$+[2N]\ A_{1g}^{(-)}$		$[2N] + \Delta S \tan\alpha$	0	0	0
N	$c - [1] + [2N-1]$	$E_{1u}^{(-)}$	$c - [1] + [2N-1] - (\Delta S/2)\tan\beta$	$m_-{}^2 \sin^2(\alpha+\beta)$	$\mu_-/2$	$B_{SG}^{N} + B_{PN}^{N} + B_{P'N}^{N}$ [e]
N′	$c + [1] - [2N-1]$	$E_{2N+1,u}^{(-)}$	$c + [1] - [2N-1] + (\Delta S/2)\tan\beta$	$m_-{}^2 \cos^2(\alpha+\beta)$	$\mu_-/2$	$B_{SG}^{N'} + B_{PN'}^{N'} + B_{P'N'}^{N'}$ [f]
P	$c + [1] + [2N-1]$	$E_{2N+1,u}^{(+)}$	$c + [1] + [2N-1] - \Delta S/2$	$m_+{}^2 \sin^2\alpha'$	$\mu_-/2$	$B_{SG}^{P} + B_{N'P}^{P} + B_{NP}^{P}$ [g]
P′	$c + [1] + [2N-1]$	$E_{1u}^{(+)}$	$c + [1] + [2N-1] + \Delta S/2$	$m_+{}^2 \cos^2\alpha'$	$\mu_-/2$	$B_{SG}^{P'} + B_{N'P'}^{P'} + B_{NP'}^{P'}$ [h]

[a] See footnote *a* in Table 3. [b] $\alpha = (1/2)\tan^{-1}(\Delta S/[2N])$; $\beta = (1/2)\tan^{-1}\{\Delta S/2([1] - [2N-1])\}$; $\alpha' = \alpha + \pi/4$; $\beta' = \beta + \pi/4$. [c] Spectroscopic characteristics of transitions from the G state. [d] See footnote *c* in Table 3. [e] $B_{SG}^{N} = -2\Delta^{-1}(S,G)\mu m_+m_-\cos\alpha\sin(\alpha+\beta)\sin\beta$; $B_{PN}^{N} = -\Delta^{-1}(P,N)[(\mu_+/2)\sin\beta' - \mu\cos\beta']m_+m_-\sin\alpha'\sin(\alpha+\beta)$; $B_{P'N}^{N} = \Delta^{-1}(P',N)[(\mu_+/2)\cos\beta' - \mu\sin\beta']m_+m_-\cos\alpha'\sin(\alpha+\beta)$. [f] $B_{SG}^{N'} = -2\Delta^{-1}(S,G)\mu m_+m_-\cos\alpha\cos(\alpha+\beta)\cos\beta$; $B_{PN'}^{N'} = -\Delta^{-1}(P,N')[(\mu_+/2)\cos\beta' + \mu\sin\beta']m_+m_-\sin\alpha'\cos(\alpha+\beta)$; $B_{P'N'}^{N'} = -\Delta^{-1}(P',N')[(\mu_+/2)\sin\beta' + \mu\cos\beta']m_+m_-\cos\alpha'\cos(\alpha+\beta)$. [g] $B_{SG}^{P} = -\Delta^{-1}(S,G)(\sqrt{2})\mu m_+m_-\sin\alpha'\cos\alpha$; $B_{N'P}^{P} = -B_{PN'}^{N'} = \Delta^{-1}(P,N')[(\mu_+/2)\cos\beta' + \mu\sin\beta']m_+m_-\sin\alpha'\cos(\alpha+\beta)$; $B_{NP}^{P} = -B_{PN}^{N} = \Delta^{-1}(P,N)[(\mu_+/2)\sin\beta' - \mu\cos\beta']m_+m_-\sin\alpha'\sin(\alpha+\beta)$. [h] $B_{SG}^{P'} = -\Delta^{-1}(S,G)(\sqrt{2})\mu m_+m_-\cos\alpha'\cos\alpha$; $B_{N'P'}^{P'} = -B_{P'N'}^{N'} = \Delta^{-1}(P',N')[(\mu_+/2)\sin\beta' + \mu\cos\beta']m_+m_-\cos\alpha'\sin(\alpha+\beta)$; $B_{NP'}^{P'} = -B_{P'N}^{N} = -\Delta^{-1}(P',N)[(\mu_+/2)\cos\beta' - \mu\sin\beta']m_+m_-\cos\alpha'\sin(\alpha+\beta)$.

results in themselves, since it permits the interpretation of spectra of numerous π systems that already are well known. As justified in Part 2, the criterion for strong perturbation is $\Delta S > 2[2N]$, and Fig. 3 shows that $[2N]$ is of the order of 1 eV. For our purposes, then, an unaromatic (or ambiaromatic) species is produced from a $4N$-electron perimeter by a perturbation that induces at least a ≈2 eV gap between the one-electron energies of the highest occupied and the lowest empty MO.

Acknowledgements

This work was supported by the National Science Foundation (CHE-9412767 and CHE-9318469). U. H. is grateful to the *Deutsche Forschungsgemeinschaft* for a scholarship.

References

1 The project was initiated at the University of Utah. For a preliminary report, see U. Höweler, P. K. Chatterjee, K. A. Klingensmith, J. Waluk and J. Michl, *Pure Appl. Chem.*, 1989, **61**, 2117.
2 J. R. Platt, *J. Chem. Phys.*, 1949, **17**, 484.
3 W. Moffitt, *J. Chem. Phys.*, 1954, **22**, 320.
4 For a more recent summary and extension to higher excited states, see G. Hohlneicher and B. Börsch-Pulm, *Ber. Bunsenges. Phys. Chem.*, 1987, **91**, 929.
5 W. Moffitt, *J. Chem. Phys.*, 1954, **22**, 1820.
6 E. Heilbronner and J. N. Murrell, *Mol. Phys.*, 1963, **6**, 1.
7 M. Gouterman, *J. Mol. Spectrosc.*, 1961, **6**, 138.
8 J. Michl, *J. Am. Chem. Soc.*, 1978, **100**, 6801.
9 J. Michl, *J. Am. Chem. Soc.*, 1978, **100**, 6812.
10 J. Michl, *J. Am. Chem. Soc.*, 1978, **100**, 6819.
11 J. Michl, *Tetrahedron*, 1984, **40**, 3845.
12 V. Bonačić-Koutecký, J. Koutecký and J. Michl, *Angew. Chem., Int. Ed. Engl.*, 1987, **26**, 170; J. Michl and V. Bonačić-Koutecký, *Tetrahedron*, 1988, **44**, 7559; J. Michl, *J. Am. Chem. Soc.*, 1996, **118**, 3568.
13 P.-O. Löwdin, *J. Chem. Phys.*, 1950, **18**, 365.
14 C. H. Martin and K. F. Freed, *J. Chem. Phys.*, 1994, **101**, 4011; *J. Phys. Chem.*, 1995, **99**, 2701.
15 L. Salem and C. Rowland, *Angew. Chem., Int. Ed. Engl.*, 1972, **11**, 92.
16 J. Michl, *Mol. Photochem.*, 1972, **4**, 257.
17 C. Doubleday, Jr., J. W. McIver, Jr. and M. Page, *J. Am. Chem. Soc.*, 1982, **104**, 6533.
18 W. T. Borden, in *Biradicals*, ed. W. T. Borden, Wiley, New York, 1982, p. 1.
19 P. N. Schatz and A. J. McCaffery, *Q. Rev. Chem. Soc.*, 1969, **23**, 552.
20 If we did not make the ZDO approximation, the lowest singlet–triplet and excited singlet degeneracies would be lifted already at the present level of CI. The off-diagonal element $\langle -N\text{-}N|NN\rangle$ between Ψ_{-N}^{N} and Ψ_{N}^{-N} listed as $[2N]$ in expression (9) would become $K'_{AB} - K_{AB}$. Here, K_{AB} is the exchange integral between the localized real orbitals $\psi_A = (\psi_N + \psi_{-N})/\sqrt{2}$ and $\psi_B = (\psi_N - \psi_{-N})/\sqrt{2}$, and $K'_{AB} = (J_{AA} + J_{BB})/4 - J_{AB}/2$, where J_{AA}, J_{BB} and J_{AB} are the Coulomb electron repulsion integrals. The energy of Ψ_0, which is also listed as $[2N]$ in the Hamiltonian matrix [eqn. (9)], would become $K_{AB} + K_{AB}$. The quantity K'_{AB} is equal to the exchange integral between the delocalized real orbitals $(\psi_A + \psi_B)/\sqrt{2}$ and $(\psi_A - \psi_B)/\sqrt{2}$. In the ZDO approximation, $K_{AB} = [2N]$ and $K_{AB} = 0$ for neutral annulenes, and this is characteristic of pair biradicals. In contrast, $K'_{AB} = K_{AB} = [2N]/2$ for charged annulenes (axial biradicals).
21 R. Pariser, *J. Chem. Phys.*, 1956, **24**, 250.
22 A. D. McLachlan, *Mol. Phys.*, 1959, **2**, 271.
23 J. Koutecký, *J. Chem. Phys.*, 1966, **44**, 3702.
24 J. Koutecký, J. Paldus and J. ČíŌek, *J. Chem. Phys.*, 1985, **83**, 1722.
25 J. Michl, *J. Chem. Phys.*, 1974, **61**, 4270.
26 P. J. Stephens, P. N. Schatz, A. B. Ritchie and A. J. McCaffery, *J. Chem. Phys.*, 1968, **48**, 132.
27 These characteristics are typical of the class of pair biradicals, to which the uncharged antiaromatic annulenes belong, and of the class of axial biradicals, to which the charged ones belong, respectively.
28 W. T. Borden, in *Biradicals*, ed. W. T. Borden, Wiley, New York, 1982, p. 58.
29 A. Castellan and J. Michl, *J. Am. Chem. Soc.*, 1978, **100**, 6824.
30 R. Pariser and R. G. Parr, *J. Chem. Phys.*, 1953, **21**, 466; J. A. Pople, *Trans. Faraday Soc.*, 1953, **49**, 1375.

Paper 8/00088C
Received 5th *January* 1998
Accepted 4th *February* 1998